

Penguin-dominated $B \rightarrow \phi K_1(1270)$ and $\phi K_1(1400)$ decays in the perturbative QCD approach

Xin Liu,^{1,*} Zhi-Tian Zou,^{2,†} and Zhen-Jun Xiao^{3,‡}

¹*School of Physics and Electronic Engineering,*

Jiangsu Normal University, Xuzhou, Jiangsu 221116, People's Republic of China

²*Department of Physics, Yantai University, Yantai, Shandong 264005, People's Republic of China*

³*Department of Physics and Institute of Theoretical Physics,*

Nanjing Normal University, Nanjing, Jiangsu 210023, People's Republic of China

(Dated: October 23, 2014)

We investigate the CP-averaged branching ratios, the polarization fractions, the relative phases, and the CP-violating asymmetries of the penguin-dominated $B \rightarrow \phi K_1(1270)$ and $\phi K_1(1400)$ decays in the perturbative QCD(pQCD) approach, where $K_1(1270)$ and $K_1(1400)$ are believed to be the mixtures of two distinct types of axial-vector $K_{1A}({}^3P_1)$ and $K_{1B}({}^1P_1)$ states with different behavior, however, their mixing angle θ_{K_1} is still a hot and controversial topic presently. By numerical evaluations with two different mixing angles $\theta_{K_1} \sim 33^\circ$ and 58° and phenomenological analysis, we find that: (a) the pQCD predictions for the branching ratio, the longitudinal polarization fraction and the direct CP violation of $B^\pm \rightarrow \phi K_1(1270)^\pm$ decay with the smaller angle 33° are in good agreement with the currently available data; (b) though the central values significantly exceed the available upper limit, both pQCD predictions of $Br(B^\pm \rightarrow \phi K_1(1400)^\pm)$ with two different mixing angles are consistent with that obtained in QCD factorization and with the preliminary data in 2σ errors. These results and other relevant predictions for the considered decays will be further tested by the LHCb and the forthcoming Super-B experiments; (c) the weak annihilation contributions can play an important role in $B \rightarrow \phi K_1(1270)$ and $\phi K_1(1400)$ decays; (d) these pQCD predictions combined with the future precision measurements can examine the reliability of the factorization approach employed here, but also explore the complicated QCD dynamics and mixing angle θ_{K_1} of the axial-vector $K_1(1270)$ and $K_1(1400)$ system.

PACS numbers: 13.25.Hw, 12.38.Bx, 14.40.Nd

I. INTRODUCTION

In the quark model, the possible quantum numbers J^{PC} for the orbitally excited axial-vector mesons are 1^{++} or 1^{+-} , depending on different spin couplings of the involved two quarks. In the SU(3) limit, those mesons can not mix with each other; but, since the s quark is heavier than u, d quarks, the physical states of strange axial-vector mesons, $K_1(1270)$ and $K_1(1400)$, are believed to be mixtures of two distinct types of K_{1A} and K_{1B} , where K_{1A} and K_{1B} are 3P_1 and 1P_1 states, respectively. Because both K_1 (Hereafter, for the sake of simplicity, we will adopt K_1 to denote $K_1(1270)$ and $K_1(1400)$ unless otherwise stated.) mesons are not pure 3P_1 or 1P_1 states, the mixing angle θ_{K_1} between two axial-vector states K_{1A} and K_{1B} is now of great interest at both theoretical and experimental aspects. Furthermore, the mixing angle θ_{K_1} can be utilized to determine the mixing angle θ_{1P_1} and θ_{3P_1} with the former(latter) being the mixing angle of $h_1(1170)(f_1(1285))$ and $h_1(1380)(f_1(1420))$ in the flavor basis through mass relations(for detail, see recent discussion [1]). However, this mixing angle θ_{K_1} is still an issue in controversy presently. It is therefore definitely interesting to investigate the mixing angle θ_{K_1} through kinds of ways, for example, examining the hints of θ_{K_1} in the rare B meson decays to the final states involving the aforementioned K_1 mesons.

Recently, the BABAR Collaboration has measured the branching ratio, the longitudinal polarization fraction and the direct CP asymmetry (Here, the definition of the direct CP asymmetry \mathcal{A}_{CP} is $\frac{\Gamma^+ - \Gamma^-}{\Gamma^+ + \Gamma^-}$ [2], where Γ^+ and Γ^- denote the decay width of B^+ and B^- meson, respectively.) of $B^\pm \rightarrow \phi K_1(1270)^\pm$ decay [2] for the first time,

$$\begin{aligned} Br(B^\pm \rightarrow \phi K_1(1270)^\pm) &= (6.1 \pm 1.6 \pm 1.1) \times 10^{-6}; \\ f_L(B^\pm \rightarrow \phi K_1(1270)^\pm) &= 0.46_{-0.13-0.07}^{+0.12+0.06}; \\ \mathcal{A}_{CP}(B^\pm \rightarrow \phi K_1(1270)^\pm) &= +0.15 \pm 0.19 \pm 0.05; \end{aligned} \quad (1)$$

and placed the upper limit at 90% C.L. on the branching ratio of $B^\pm \rightarrow \phi K_1(1400)^\pm$ decay [2],

$$Br(B^\pm \rightarrow \phi K_1(1400)^\pm) < 3.2(0.3 \pm 1.6 \pm 0.7) \times 10^{-6}. \quad (2)$$

* Electronic address: liuxin.physics@gmail.com

† Electronic address: zouzt@ytu.edu.cn

‡ Electronic address: xiaozhenjun@njnu.edu.cn

One can easily observe that the vector-axial-vector $B^\pm \rightarrow \phi K_1(1270)^\pm$ decay looks more like the vector-vector $B^\pm \rightarrow \phi K^{*\pm}$ one, which has been confirmed experimentally that the transverse amplitudes account for a large fraction [3–8]. The precision of above measurements for $B^\pm \rightarrow \phi K_1(1270)^\pm$ will be improved rapidly in the relevant Large Hadron Collider beauty (LHCb) experiments. Moreover, the observation on the $B^0 \rightarrow \phi K_1(1270)^0$ and $B \rightarrow \phi K_1(1400)$ decays could also be made with good precision at LHCb in the near future.

It is well known that the study of exclusive non-leptonic weak decays of B mesons provides not only good opportunities for testing the standard model(SM) but also powerful means for probing different new physics scenarios beyond the SM. Just like the two body charmless hadronic $B \rightarrow VV$ decays, $B \rightarrow VA$ modes are also expected to have rich physics as they have three polarization states. Through polarization studies, these channels can shed light on the underlying helicity structure of the decay mechanism [9]. Experimentally, measurements of polarization in rare vector-vector B meson decay, such as $B \rightarrow \phi K^*$, have revealed an unexpectedly large fraction of transverse polarization, which violates the naively expected hierarchy, i.e., $f_L \sim 1$ and $f_\parallel \approx f_\perp \sim \mathcal{O}(m_V^2/m_B^2)$, with f_L , f_\parallel , and f_\perp denoting the polarization fractions on longitudinal, parallel, and perpendicular polarization, respectively. In view of the polarization anomalies exhibited in $B \rightarrow \phi K^*$ decays and the same transition pattern $b \rightarrow \bar{s}s\bar{s}$ involved in both $B \rightarrow \phi K^*$ and $B \rightarrow \phi K_1$ decays, it is of particular interest to see whether similar anomalies occur in $B \rightarrow \phi K_1$ decays. Moreover, in order to find out the real causes of the above mentioned polarization anomalies in these types of decays, it demands considerable studies on more processes.

At the theoretical aspect, up to now, the two-body hadronic $B \rightarrow \phi K_1$ decays have been investigated by G. Calderón *et al.* [10] in naive factorization approach, by Chen *et al.* [11] in generalized factorization approach(GFA), and by Cheng and Yang [9] in QCD factorization(QCDF), respectively. The theoretical predictions were given with the mixing angle $\theta_{K_1} \approx 32^\circ, 58^\circ$ in Ref. [10] and $\theta_{K_1} \approx 37^\circ, 58^\circ$ in Refs. [9, 11]. However, those predictions of the decay rates and polarization fractions for the considered $B \rightarrow \phi K_1$ decays presented very different phenomenologies. For the case of $B^+ \rightarrow \phi K_1(1270)^+$ decay, for instance, the authors of Ref. [10] found that the branching ratio of the considered decay is in the order of $10^{-9} \sim 10^{-7}$, which is much smaller than currently available data. Furthermore, the numerical results were also very sensitive to the variation of the mixing angle θ_{K_1} : $Br(B^+ \rightarrow \phi K_1(1270)^+) \sim 4 \times 10^{-9}$ or 3×10^{-7} for $\theta_{K_1} \approx 32^\circ$ or 58° , respectively. The relevant polarization fractions were not evaluated in Ref. [10]. By neglecting the so-called negligible annihilation contributions, the authors of Ref. [11] predicted the branching ratio $Br(B^+ \rightarrow \phi K_1(1270)^+) \sim 10^{-5}$ with the preferred $N_c^{\text{eff}} = 2$ or 3, where N_c^{eff} was the effective color number containing the non-factorizable effects. When N_c^{eff} is close to 5, the numerical results for the decay rate with mixing angle 37° and 58° are well consistent with the present measurement. Moreover, the calculations showed the moderate dependence on the mixing angle θ_{K_1} and preferred the smaller angle for the $B^+ \rightarrow \phi K_1(1270)^+$ mode. And the longitudinal polarization fractions were predicted around 90% in the cases of both 37° and 58° . By using the light-cone QCD sum rule results for the $B \rightarrow K_{1A}$ and $B \rightarrow K_{1B}$ form factors [9], the authors predicted the branching ratios and polarization fractions in QCDF by adopting the penguin-annihilation parameters inferred from the $B \rightarrow \phi K^*$ decays. The decay rate for $B^+ \rightarrow \phi K_1(1270)^+$ mode is $(3.8_{-3.4}^{+5.4}) \times 10^{-6}$ with $\theta_{K_1} \approx 37^\circ$ and $(3.4_{-3.2}^{+5.9}) \times 10^{-6}$ with $\theta_{K_1} \approx 58^\circ$, respectively, which is consistent with the data within errors and shows the weak dependence on the mixing angle θ_{K_1} . While the predicted longitudinal polarization fractions exhibit the dominant longitudinal(transverse) contributions for $B^+ \rightarrow \phi K_1(1270)^+$ with mixing angle $\theta_{K_1} \approx 37^\circ(58^\circ)$. Frankly speaking, the large discrepancies among those predicted branching ratios and polarization fractions of the considered decays indicate that more studies by employing new approaches and/or methods are greatly needed to explore these decay modes and understand in depth the physics hidden in them.

In this work, we will calculate the CP-averaged branching ratios, the polarization fractions, the relative phases, and the CP-violating asymmetries of the four charmless hadronic $B \rightarrow \phi K_1$ decays¹ by employing the low energy effective Hamiltonian [14] and the perturbative QCD (pQCD) factorization approach[15–18] based on the k_T factorization theorem. By keeping the transverse momentum k_T of the quarks, the pQCD approach is free of endpoint singularity and the Sudakov formalism makes it more self-consistent. In the pQCD approach, we can explicitly evaluate not only the factorizable and non-factorizable spectator diagrams, but also the weak annihilation ones. Although there is a different viewpoint on the evaluations of annihilation diagrams proposed in the soft-collinear effective theory (See Refs. [19, 20] for details), the previous predictions on the annihilation contributions in heavy flavor B meson decays calculated with the pQCD approach have already been tested at various aspects, for example, branching ratios of pure annihilation $B_d \rightarrow D_s^- K^+$, $B_d \rightarrow K^+ K^-$, and $B_s \rightarrow \pi^+ \pi^-$ decays [21–24], direct CP asymmetries of $B^0 \rightarrow \pi^+ \pi^-$, $K^+ \pi^-$ decays [15–17, 25], and the explanation of $B \rightarrow \phi K^*$ polarization problem [26, 27], which indicate that the pQCD approach is a reliable method to deal with the annihilation diagrams.

The paper is organized as follows. In Sec. II, we present the formalism, hadron wave functions and perturbative calculations of the considered four $B \rightarrow \phi K_1$ decays. The numerical results and the corresponding phenomenological analyses are addressed in Sec. III. Finally, Sec. IV contains the main conclusions and a short summary.

¹ These considered $B \rightarrow \phi K_1$ decays are analogous to vector-vector $B \rightarrow \phi K^*$ decays, which are expected to arise only from virtual loop effects in the standard model and are particularly sensitive to the contributions from beyond the standard model [12, 13]. Moreover, some physical quantities such as the relative phases and the CP-violating asymmetries of $B \rightarrow \phi K_1$ decays are evaluated for the first time in this work.

II. FORMALISM

The pQCD approach is one of the popular methods to evaluate the hadronic matrix elements in the heavy b -flavor mesons' decays. The basic idea of the pQCD approach is that it takes into account the transverse momentum k_T of the valence quarks in the calculation of the hadronic matrix elements. The B meson transition form factors, and the non-factorizable spectator and annihilation contributions are then all calculable in the framework of the k_T factorization, where three energy scales m_W, m_B and $t \approx \sqrt{m_B \Lambda_{\text{QCD}}}$ are involved [15–17, 28–30]. The running of the Wilson coefficients $C_i(t)$ with $t \geq \sqrt{m_B \Lambda_{\text{QCD}}}$ are controlled by the renormalization group equation and can be calculated perturbatively. The dynamics below $\sqrt{m_B \Lambda_{\text{QCD}}}$ is soft, which is described by the meson wave functions. The soft dynamics is not perturbative but universal for all channels.

In the pQCD approach, the amplitude of $B \rightarrow \phi K_1$ decays can therefore be factorized into the convolution of the six-quark hard kernel(H), the jet function(J) and the Sudakov factor(S) with the bound-state wave functions(Φ) as follows,

$$A(B \rightarrow \phi K_1) = \Phi_B \otimes H \otimes J \otimes S \otimes \Phi_\phi \otimes \Phi_{K_1}, \quad (3)$$

The function Φ is the wave function describing hadronization of the quark and anti-quark to the meson, which is independent of the specific processes and usually determined by employing nonperturbative QCD techniques or other well measured processes. The jet function J comes from the threshold resummation, which exhibits strong suppression effect in the small x (quark momentum fraction) region [31, 32]. The Sudakov factor S comes from the k_T resummation, which provide a strong suppression in the small k_T region [33, 34]. These resummation effects therefore guarantee the removal of the endpoint singularities.

Because of the rather heavy b quark, for convenience, we usually work in the rest frame of B meson. By utilizing the light-cone coordinate (P^+, P^-, \mathbf{P}_T) to describe the meson's momenta with the definitions

$$P^\pm = \frac{p_0 \pm p_3}{\sqrt{2}} \quad \text{and} \quad \mathbf{P}_T = (p_1, p_2); \quad (4)$$

we can write the involved three meson momenta in the $B \rightarrow \phi K_1$ decays,

$$P_1 = \frac{m_B}{\sqrt{2}}(1, 1, \mathbf{0}_T), \quad P_2 = \frac{m_B}{\sqrt{2}}(1 - r_3^2, r_2^2, \mathbf{0}_T), \quad P_3 = \frac{m_B}{\sqrt{2}}(r_3^2, 1 - r_2^2, \mathbf{0}_T), \quad (5)$$

respectively, where the ϕ (K_1) meson moves in the plus (minus) z direction carrying the momentum P_2 (P_3) and $r_2 = m_\phi/m_B$, $r_3 = m_{K_1}/m_B$. When we choose the (light) quark momenta in B , ϕ and K_1 mesons as k_1 , k_2 , and k_3 , respectively, and define

$$k_1 = (x_1 P_1^+, 0, \mathbf{k}_{1T}), \quad k_2 = x_2 P_2 + (0, 0, \mathbf{k}_{2T}), \quad k_3 = x_3 P_3 + (0, 0, \mathbf{k}_{3T}). \quad (6)$$

then integrate out k_1^- , k_2^- , and k_3^+ in the Eq.(3), the more explicit form of the decay amplitude for $B \rightarrow \phi K_1$ decays can be conceptually rewritten as the following,

$$A(B \rightarrow \phi K_1) \sim \int dx_1 dx_2 dx_3 b_1 db_1 b_2 db_2 b_3 db_3 \cdot \text{Tr} \left[C(t) \Phi_B(x_1, b_1) \Phi_\phi(x_2, b_2) \Phi_{K_1}(x_3, b_3) H(x_i, b_i, t) S_t(x_i) e^{-S(t)} \right]. \quad (7)$$

where b_i is the conjugate space coordinate of k_{iT} , and t is the largest energy scale in hard kernel $H(x_i, b_i, t)$. Tr denotes the trace over Dirac and color indices. $C(t)$ stands for the Wilson coefficients including the large logarithms $\ln(m_W/t)$. $S_t(x_i)$ and $e^{-S(t)}$ correspond to the jet function J and Sudakov factor S in Eq. (3), respectively, whose detailed expressions can be easily found in the original Refs. [31–34]. Thus, with Eq. (7), we can give the convoluted amplitudes of the $B \rightarrow \phi K_1$ decays, which will be presented in the next section, through the evaluations of the hard kernel $H(x_i, b_i, t)$ at leading order in α_s expansion in the pQCD approach.

A. Wave functions and distribution amplitudes

The heavy B meson is usually treated as a heavy-light system and its light-cone wave function can generally be defined as [15–17, 35]

$$\begin{aligned} \Phi_{B, \alpha\beta, ij} &\equiv \langle 0 | \bar{b}_{\beta j}(0) q_{\alpha i}(z) | B(P) \rangle \\ &= \frac{i\delta_{ij}}{\sqrt{2N_c}} \int dx d^2 k_T e^{-i(xP^- z^+ - k_T z_T)} \{ (P^+ m_B) \gamma_5 \phi_B(x, k_T) \}_{\alpha\beta}; \end{aligned} \quad (8)$$

where the indices i, j and α, β are the Lorentz indices and color indices respectively, $P(m)$ is the momentum(mass) of the B meson, N_c is the color factor, and k_T is the intrinsic transverse momentum of the light quark in B meson.

In Eq. (8), $\phi_B(x, k_T)$ is the B meson distribution amplitude and obeys to the following normalization condition,

$$\int_0^1 dx \phi_B(x, b=0) = \frac{f_B}{2\sqrt{2N_c}}. \quad (9)$$

where b is the conjugate space coordinate of transverse momentum k_T and f_B is the decay constant of B meson. For B meson, the distribution amplitude in the impact b space has been proposed

$$\phi_B(x, b) = N_B x^2 (1-x)^2 \exp \left[-\frac{1}{2} \left(\frac{x m_B}{\omega_b} \right)^2 - \frac{\omega_b^2 b^2}{2} \right], \quad (10)$$

in Refs. [15–17], where the normalization factor N_B is related to the decay constant f_B through Eq. (9). The shape parameter ω_b has been fixed at $\omega_b = 0.40 \pm 0.04$ GeV by using the rich experimental data on the B mesons with $f_B = 0.19$ GeV based on lots of calculations of form factors [35] and other well-known decay modes of B mesons [15–17] in the pQCD approach in recent years.

The light-cone wave functions of the vector meson ϕ and axial-vector state $K_{1A(B)}$ have been given in the QCD sum rule method up to twist-3 as [36, 37]

$$\begin{aligned} \Phi_{\phi, \alpha\beta, ij}^L &\equiv \langle \phi(P, \epsilon_L) | \bar{q}(z)_{\beta j} q(0)_{\alpha i} | 0 \rangle \\ &= \frac{\delta_{ij}}{\sqrt{2N_c}} \int_0^1 dx e^{ixP \cdot z} \left\{ m_\phi \not{\epsilon}_L \phi_\phi(x) + \not{\epsilon}_L \not{P} \phi_\phi^t(x) + m_\phi \phi_\phi^s(x) \right\}_{\alpha\beta}, \end{aligned} \quad (11)$$

$$\begin{aligned} \Phi_{\phi, \alpha\beta, ij}^T &\equiv \langle \phi(P, \epsilon_T) | \bar{q}(z)_{\beta j} q(0)_{\alpha i} | 0 \rangle \\ &= \frac{\delta_{ij}}{\sqrt{2N_c}} \int_0^1 dx e^{ixP \cdot z} \left\{ m_\phi \not{\epsilon}_T \phi_\phi^v(x) + \not{\epsilon}_T \not{P} \phi_\phi^T(x) + m_\phi i \epsilon_{\mu\nu\rho\sigma} \gamma_5 \gamma^\mu \not{\epsilon}_T^\nu n^\rho v^\sigma \phi_\phi^a(x) \right\}_{\alpha\beta}, \end{aligned} \quad (12)$$

and [38, 39]

$$\begin{aligned} \Phi_{K_{1A(B)}, \alpha\beta, ij}^L &\equiv \langle K_{1A(B)}(P, \epsilon_L) | \bar{q}(z)_{\beta j} q(0)_{\alpha i} | 0 \rangle \\ &= \frac{\delta_{ij} \gamma_5}{\sqrt{2N_c}} \int_0^1 dx e^{ixP \cdot z} \left\{ m_{K_{1A(B)}} \not{\epsilon}_L \phi_{K_{1A(B)}}(x) + \not{\epsilon}_L \not{P} \phi_{K_{1A(B)}}^t(x) + m_{K_{1A(B)}} \phi_{K_{1A(B)}}^s(x) \right\}_{\alpha\beta}, \end{aligned} \quad (13)$$

$$\begin{aligned} \Phi_{K_{1A(B)}, \alpha\beta, ij}^T &\equiv \langle K_{1A(B)}(P, \epsilon_T) | \bar{q}(z)_{\beta j} q(0)_{\alpha i} | 0 \rangle \\ &= \frac{\delta_{ij} \gamma_5}{\sqrt{2N_c}} \int_0^1 dx e^{ixP \cdot z} \left\{ m_{K_{1A(B)}} \not{\epsilon}_T \phi_{K_{1A(B)}}^v(x) + \not{\epsilon}_T \not{P} \phi_{K_{1A(B)}}^T(x) \right. \\ &\quad \left. + m_{K_{1A(B)}} i \epsilon_{\mu\nu\rho\sigma} \gamma_5 \gamma^\mu \not{\epsilon}_T^\nu n^\rho v^\sigma \phi_{K_{1A(B)}}^a(x) \right\}_{\alpha\beta}, \end{aligned} \quad (14)$$

for longitudinal polarization and transverse polarization, respectively, with the polarization vectors ϵ_L and ϵ_T of ϕ or $K_{1A(B)}$, satisfying $P \cdot \epsilon = 0$, where x denotes the momentum fraction carried by quark in the meson, and $n = (1, 0, \mathbf{0}_T)$ and $v = (0, 1, \mathbf{0}_T)$ are dimensionless light-like unit vectors. We adopt the convention $\epsilon^{0123} = 1$ for the Levi-Civita tensor $\epsilon^{\mu\nu\alpha\beta}$.

The twist-2 distribution amplitudes ϕ_ϕ and ϕ_ϕ^T can be parameterized as:

$$\phi_\phi(x) = \frac{f_\phi}{2\sqrt{2N_c}} 6x(1-x) \left[1 + a_{2\phi}^\parallel \frac{3}{2} (5(2x-1)^2 - 1) \right], \quad (15)$$

$$\phi_\phi^T(x) = \frac{f_\phi^T}{2\sqrt{2N_c}} 6x(1-x) \left[1 + a_{2\phi}^\perp \frac{3}{2} (5(2x-1)^2 - 1) \right], \quad (16)$$

Here f_ϕ and f_ϕ^T are the decay constants of the ϕ meson with longitudinal and transverse polarization, respectively, whose values are [40, 41]

$$f_\phi = 0.231 \pm 0.004 \quad \text{GeV}, \quad f_\phi^T = 0.200 \pm 0.010 \quad \text{GeV}. \quad (17)$$

The Gegenbauer moments $a_{2\phi}^{\parallel, \perp}$ are mainly determined by the technique of QCD sum rules. Here we quote the recent updates [37, 41] as

$$a_{2\phi}^\parallel = 0.18 \pm 0.08, \quad a_{2\phi}^\perp = 0.14 \pm 0.07, \quad (18)$$

where the values are taken at $\mu = 1$ GeV.

The asymptotic forms of the twist-3 distribution amplitudes $\phi_\phi^{t,s}$ and $\phi_\phi^{v,a}$ are adopted:

$$\phi_\phi^t(x) = \frac{3f_\phi^T}{2\sqrt{2N_c}}(2x-1)^2, \quad \phi_\phi^s(x) = -\frac{3f_\phi^T}{2\sqrt{2N_c}}(2x-1), \quad (19)$$

$$\phi_\phi^v(x) = \frac{3f_\phi}{8\sqrt{2N_c}}(1+(2x-1)^2), \quad \phi_\phi^a(x) = -\frac{3f_\phi}{4\sqrt{2N_c}}(2x-1). \quad (20)$$

For the axial-vector meson $K_{1A(B)}$, its twist-2 light-cone distribution amplitudes can generally be expanded as the Gegenbauer polynomials [38]:

$$\phi_{K_{1A(B)}}(x) = \frac{f_{K_{1A(B)}}}{2\sqrt{2N_c}}6x(1-x) \left[a_{0K_{1A(B)}}^\parallel + 3a_{1K_{1A(B)}}^\parallel(2x-1) + a_{2K_{1A(B)}}^\parallel \frac{3}{2}(5(2x-1)^2-1) \right], \quad (21)$$

$$\phi_{K_{1A(B)}}^T(x) = \frac{f_{K_{1A(B)}}}{2\sqrt{2N_c}}6x(1-x) \left[a_{0K_{1A(B)}}^\perp + 3a_{1K_{1A(B)}}^\perp(2x-1) + a_{2K_{1A(B)}}^\perp \frac{3}{2}(5(2x-1)^2-1) \right], \quad (22)$$

For twist-3 light-cone distribution amplitudes, we use the following form as in Ref. [39]:

$$\phi_{K_{1A(B)}}^s(x) = \frac{f_{K_{1A(B)}}}{4\sqrt{2N_c}} \frac{d}{dx} \left[6x(1-x)(a_{0K_{1A(B)}}^\perp + a_{1K_{1A(B)}}^\perp(2x-1)) \right], \quad (23)$$

$$\phi_{K_{1A(B)}}^t(x) = \frac{f_{K_{1A(B)}}}{2\sqrt{2N_c}} \left[3a_{0K_{1A(B)}}^\perp(2x-1)^2 + \frac{3}{2}a_{1K_{1A(B)}}^\perp(2x-1)(3(2x-1)^2-1) \right], \quad (24)$$

$$\phi_{K_{1A(B)}}^v(x) = \frac{f_{K_{1A(B)}}}{2\sqrt{2N_c}} \left[\frac{3}{4}a_{0K_{1A(B)}}^\parallel(1+(2x-1)^2) + \frac{3}{2}a_{1K_{1A(B)}}^\parallel(2x-1)^3 \right], \quad (25)$$

$$\phi_{K_{1A(B)}}^a(x) = \frac{f_{K_{1A(B)}}}{8\sqrt{2N_c}} \frac{d}{dx} \left[6x(1-x)(a_{0K_{1A(B)}}^\parallel + a_{1K_{1A(B)}}^\parallel(2x-1)) \right]. \quad (26)$$

where $f_{K_{1A(B)}}$ is the “normalization” constant for both longitudinally and transversely polarized mesons and the Gegenbauer moments are quoted from Ref. [38]

- For K_{1A} state,

$$\begin{aligned} a_0^\parallel &= 1, & a_1^\parallel &= -0.30_{-0.20}^{+0.00}, & a_2^\parallel &= -0.05_{-0.03}^{+0.03}; \\ a_0^\perp &= 0.27_{-0.17}^{+0.03}, & a_1^\perp &= -1.08_{-0.48}^{+0.48}, & a_2^\perp &= 0.02_{-0.21}^{+0.21}; \end{aligned} \quad (27)$$

- For K_{1B} state,

$$\begin{aligned} a_0^\parallel &= -0.19_{-0.07}^{+0.07}, & a_1^\parallel &= -1.95_{-0.45}^{+0.45}, & a_2^\parallel &= 0.10_{-0.19}^{+0.15}; \\ a_0^\perp &= 1, & a_1^\perp &= 0.30_{-0.33}^{+0.00}, & a_2^\perp &= -0.02_{-0.22}^{+0.22}. \end{aligned} \quad (28)$$

where the values are taken at $\mu = 1$ GeV. Since $f_{K_{1A}}^\perp$ and $f_{K_{1B}}$ are G-parity-violating quantities, their signs have to be flipped from particle to antiparticle due to the G parity, for example, $f_{K_{1B}^+} = -f_{K_{1B}^-}$. In the present work, the G-parity violating parameters, e.g. $a_1^{\parallel, K_{1A}}$, $a_{0,2}^{\perp, K_{1A}}$, $a_1^{\perp, K_{1B}}$ and $a_{0,2}^{\parallel, K_{1B}}$, are considered for mesons containing a strange quark.

It is worth of mentioning that the k_T dependence of the distribution amplitudes in the final states has been neglected, since its contribution is very small as indicated in Refs. [28–30]. The underlying reason is that the contribution from k_T correlated with a soft dynamics is strongly suppressed by the Sudakov effect through resummation for the wave function, which is dominated by a collinear dynamics.

B. Perturbative calculations in pQCD approach

For the considered $B \rightarrow \phi K_1$ decays induced by the $\bar{b} \rightarrow \bar{s}s\bar{s}$ transitions at the quark level, the related weak effective Hamiltonian H_{eff} [14] can be written as

$$H_{\text{eff}} = \frac{G_F}{\sqrt{2}} \left\{ V_{ub}^* V_{us} [C_1(\mu) O_1^u(\mu) + C_2(\mu) O_2^u(\mu)] - V_{tb}^* V_{ts} \left[\sum_{i=3}^{10} C_i(\mu) O_i(\mu) \right] \right\} + \text{H.c.}, \quad (29)$$

with the Fermi constant $G_F = 1.16639 \times 10^{-5} \text{GeV}^{-2}$, Cabibbo-Kobayashi-Maskawa(CKM) matrix elements V , and Wilson coefficients $C_i(\mu)$ at the renormalization scale μ . The local four-quark operators $O_i(i = 1, \dots, 10)$ are written as

(1) current-current(tree) operators

$$O_1^u = (\bar{s}_\alpha u_\beta)_{V-A} (\bar{u}_\beta b_\alpha)_{V-A}, \quad O_2^u = (\bar{s}_\alpha u_\alpha)_{V-A} (\bar{u}_\beta b_\beta)_{V-A}; \quad (30)$$

(2) QCD penguin operators

$$\begin{aligned} O_3 &= (\bar{s}_\alpha b_\alpha)_{V-A} \sum_{q'} (\bar{q}'_\beta q'_\beta)_{V-A}, \quad O_4 = (\bar{s}_\alpha b_\beta)_{V-A} \sum_{q'} (\bar{q}'_\beta q'_\alpha)_{V-A}, \\ O_5 &= (\bar{s}_\alpha b_\alpha)_{V-A} \sum_{q'} (\bar{q}'_\beta q'_\beta)_{V+A}, \quad O_6 = (\bar{s}_\alpha b_\beta)_{V-A} \sum_{q'} (\bar{q}'_\beta q'_\alpha)_{V+A}; \end{aligned} \quad (31)$$

(3) electroweak penguin operators

$$\begin{aligned} O_7 &= \frac{3}{2} (\bar{s}_\alpha b_\alpha)_{V-A} \sum_{q'} e_{q'} (\bar{q}'_\beta q'_\beta)_{V+A}, \quad O_8 = \frac{3}{2} (\bar{s}_\alpha b_\beta)_{V-A} \sum_{q'} e_{q'} (\bar{q}'_\beta q'_\alpha)_{V+A}, \\ O_9 &= \frac{3}{2} (\bar{s}_\alpha b_\alpha)_{V-A} \sum_{q'} e_{q'} (\bar{q}'_\beta q'_\beta)_{V-A}, \quad O_{10} = \frac{3}{2} (\bar{s}_\alpha b_\beta)_{V-A} \sum_{q'} e_{q'} (\bar{q}'_\beta q'_\alpha)_{V-A}. \end{aligned} \quad (32)$$

with the color indices α, β and the notations $(\bar{q}' q')_{V \pm A} = \bar{q}' \gamma_\mu (1 \pm \gamma_5) q'$. The index q' in the summation of the above operators runs through u, d, s, c , and b .

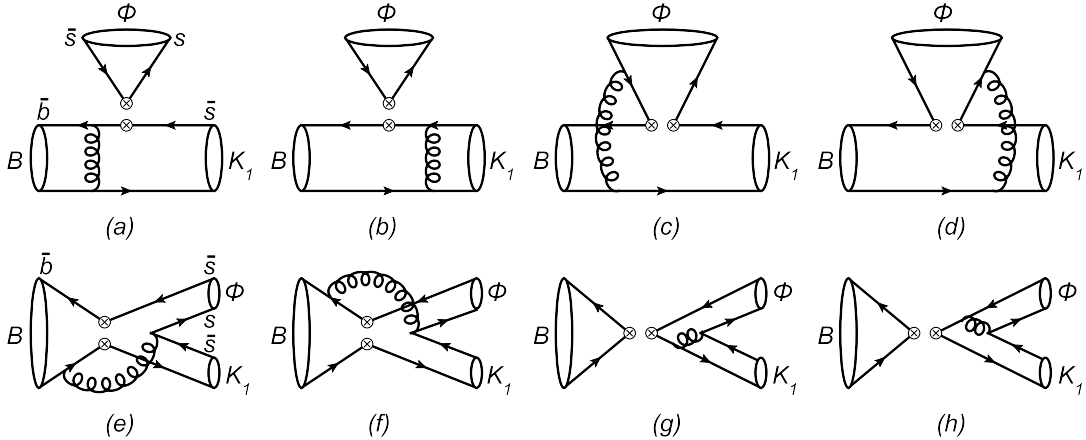


FIG. 1. Typical Feynman diagrams contributing to the penguin-dominated $B \rightarrow \phi K_1$ decays in the pQCD approach at leading order, in which K_1 stands for the axial-vector $K_1(1270)$ and $K_1(1400)$, respectively.

From the effective Hamiltonian (29), there are eight types of diagrams contributing to the $B \rightarrow \phi K_1$ decays in the pQCD approach at leading order as illustrated in Fig. 1. Analogous to the $B \rightarrow \phi K^*$ decays [42], we calculate the contributions arising from various operators as shown in Eqs. (30)-(32). Hereafter, for the sake of simplicity, we will use F and M to describe the factorizable and non-factorizable amplitudes induced by the $(V-A)(V-A)$ operators, F^{P_1} and M^{P_1} to describe the factorizable and non-factorizable amplitudes arising from the $(V-A)(V+A)$ operators, and F^{P_2} and M^{P_2} to describe the factorizable and non-factorizable amplitudes coming from the $(S-P)(S+P)$ operators that obtained by making Fierz transformation from the $(V-A)(V+A)$ operators, respectively.

For the factorizable emission(fe) diagrams 1(a) and 1(b), the corresponding Feynman amplitudes with one longitudinal polarization(L) and two transverse polarizations(N and T) can be read as follows,

$$\begin{aligned} F_{fe}^L &= -8\pi C_F m_B^2 \int_0^1 dx_1 dx_3 \int_0^\infty b_1 db_1 b_3 db_3 \phi_B(x_1, b_1) \{ [(1+x_3)\phi_3(x_3) + r_3(1-2x_3) \\ &\quad \times (\phi_3^t(x_3) + \phi_3^s(x_3))] E_{fe}(t_a) h_{fe}(x_1, x_3, b_1, b_3) + 2r_3 \phi_3^s(x_3) E_{fe}(t_b) h_{fe}(x_3, x_1, b_3, b_1) \}, \end{aligned} \quad (33)$$

$$F_{fe}^N = -8\pi C_F m_B^2 \int_0^1 dx_1 dx_3 \int_0^\infty b_1 db_1 b_3 db_3 \phi_B(x_1, b_1) r_2 \{ [\phi_3^T(x_3) + 2r_3 \phi_3^v(x_3) + r_3 x_3 \times (\phi_3^v(x_3) - \phi_3^a(x_3))] E_{fe}(t_a) h_{fe}(x_1, x_3, b_1, b_3) + r_3 [\phi_3^v(x_3) + \phi_3^a(x_3)] E_{fe}(t_b) h_{fe}(x_3, x_1, b_3, b_1) \} , \quad (34)$$

$$F_{fe}^T = -16\pi C_F m_B^2 \int_0^1 dx_1 dx_3 \int_0^\infty b_1 db_1 b_3 db_3 \phi_B(x_1, b_1) r_2 \{ [\phi_3^T(x_3) + 2r_3 \phi_3^a(x_3) - r_3 x_3 \times (\phi_3^v(x_3) - \phi_3^a(x_3))] E_{fe}(t_a) h_{fe}(x_1, x_3, b_1, b_3) + r_3 [\phi_3^v(x_3) + \phi_3^a(x_3)] E_{fe}(t_b) h_{fe}(x_3, x_1, b_3, b_1) \} ; \quad (35)$$

where ϕ_3 denotes the distribution amplitude of the axial-vector state K_{1A} or K_{1B} and $C_F = 4/3$ is a color factor. The hard functions h_i , the running hard scales t_i and the convolution functions $E_i(t)$ can be referred to Ref. [42].

Since only the vector part of $(V + A)$ current contributes to the vector meson production, $\langle A|V - A|B \rangle \langle \phi|V + A|0 \rangle = \langle A|V - A|B \rangle \langle \phi|V - A|0 \rangle$, that is

$$F_{fe}^{P_1} = F_{fe} . \quad (36)$$

For the non-factorizable emission(nfe) diagrams 1(c) and 1(d), the corresponding Feynman amplitudes are

$$M_{nfe}^L = -\frac{16\sqrt{6}}{3} \pi C_F m_B^2 \int_0^1 dx_1 dx_2 dx_3 \int_0^\infty b_1 db_1 b_2 db_2 \phi_B(x_1, b_1) \phi_2(x_2) \{ [(1-x_2)\phi_3(x_3) + r_3 x_3 (\phi_3^t(x_3) - \phi_3^s(x_3))] E_{nfe}(t_c) h_{nfe}^c(x_1, x_2, x_3, b_1, b_2) - [(x_2 + x_3)\phi_3(x_3) - r_3 x_3 (\phi_3^t(x_3) + \phi_3^s(x_3))] E_{nfe}(t_d) h_{nfe}^d(x_1, x_2, x_3, b_1, b_2) \} , \quad (37)$$

in which ϕ_2 stands for the distribution amplitude of ϕ meson.

$$M_{nfe}^N = \frac{16\sqrt{6}}{3} \pi C_F m_B^2 \int_0^1 dx_1 dx_2 dx_3 \int_0^\infty b_1 db_1 b_2 db_2 \phi_B(x_1, b_1) r_2 \{ (1-x_2)(\phi_2^v(x_2) + \phi_2^a(x_2)) \times \phi_3^T(x_3) h_{nfe}^c(x_1, x_2, x_3, b_1, b_2) E_{nfe}(t_c) + [x_2(\phi_2^v(x_2) + \phi_2^a(x_2))\phi_3^T(x_3) - 2r_3(x_2 + x_3)(\phi_2^v(x_2)\phi_3^v(x_3) + \phi_2^a(x_2)\phi_3^a(x_3))] E_{nfe}(t_d) h_{nfe}^d(x_1, x_2, x_3, b_1, b_2) \} , \quad (38)$$

$$M_{nfe}^T = -\frac{32\sqrt{6}}{3} \pi C_F m_B^2 \int_0^1 dx_1 dx_2 dx_3 \int_0^\infty b_1 db_1 b_2 db_2 \phi_B(x_1, b_1) r_2 \{ (1-x_2)(\phi_2^v(x_2) + \phi_2^a(x_2)) \times \phi_3^T(x_3) h_{nfe}^c(x_1, x_2, x_3, b_1, b_2) E_{nfe}(t_c) + [x_2(\phi_2^v(x_2) + \phi_2^a(x_2))\phi_3^T(x_3) - 2r_3(x_2 + x_3)(\phi_2^v(x_2)\phi_3^a(x_3) + \phi_2^a(x_2)\phi_3^v(x_3))] E_{nfe}(t_d) h_{nfe}^d(x_1, x_2, x_3, b_1, b_2) \} . \quad (39)$$

$$M_{nfe}^{P_1, L} = -\frac{16\sqrt{6}}{3} \pi C_F m_B^2 \int_0^1 dx_1 dx_2 dx_3 \int_0^\infty b_1 db_1 b_2 db_2 \phi_B(x_1, b_1) r_2 \{ [(1-x_2)(\phi_2^t(x_2) + \phi_2^s(x_2)) \times \phi_3(x_3) - r_3(1-x_2)(\phi_2^t(x_2) + \phi_2^s(x_2))(\phi_3^t(x_3) - \phi_3^s(x_3)) - r_3 x_3(\phi_2^t(x_2) - \phi_2^s(x_2)) \times (\phi_3^t(x_3) + \phi_3^s(x_3))] E_{nfe}(t_c) h_{nfe}^c(x_1, x_2, x_3, b_1, b_2) + [x_2(\phi_2^t(x_2) - \phi_2^s(x_2))\phi_3(x_3) - r_3 x_2(\phi_2^t(x_2) - \phi_2^s(x_2))(\phi_3^t(x_3) - \phi_3^s(x_3)) - r_3 x_3(\phi_2^t(x_2) + \phi_2^s(x_2))(\phi_3^t(x_3) + \phi_3^s(x_3))] \times E_{nfe}(t_d) h_{nfe}^d(x_1, x_2, x_3, b_1, b_2) \} , \quad (40)$$

$$M_{nfe}^{P_1, N} = -\frac{16\sqrt{6}}{3} \pi C_F m_B^2 \int_0^1 dx_1 dx_2 dx_3 \int_0^\infty b_1 db_1 b_2 db_2 \phi_B(x_1, b_1) r_3 x_3 \phi_2^T(x_2) (\phi_3^v(x_3) - \phi_3^a(x_3)) \times \{ E_{nfe}(t_c) h_{nfe}^c(x_1, x_2, x_3, b_1, b_2) + E_{nfe}(t_d) h_{nfe}^d(x_1, x_2, x_3, b_1, b_2) \} , \quad (41)$$

$$M_{nfe}^{P_1, T} = 2M_{nfe}^{P_1, N} , \quad (42)$$

$$M_{nfe}^{P_2, L} = -\frac{16\sqrt{6}}{3} \pi C_F m_B^2 \int_0^1 dx_1 dx_2 dx_3 \int_0^\infty b_1 db_1 b_2 db_2 \phi_B(x_1, b_1) \phi_2(x_2) \{ [(1-x_2+x_3)\phi_3(x_3) - r_3 x_3(\phi_3^t(x_3) + \phi_3^s(x_3))] E_e(t_c) h_{nfe}^c(x_1, x_2, x_3, b_1, b_2) - h_{nfe}^d(x_1, x_2, x_3, b_1, b_2) E_{nfe}(t_d) \times [x_2 \phi_3(x_3) + r_3 x_3(\phi_3^t(x_3) - \phi_3^s(x_3))] \} , \quad (43)$$

$$\begin{aligned}
M_{nfe}^{P_2,N} = & \frac{16\sqrt{6}}{3}\pi C_F m_B^2 \int_0^1 dx_1 dx_2 dx_3 \int_0^\infty b_1 db_1 b_2 db_2 \phi_B(x_1, b_1) r_2 \{ [(1-x_2)(\phi_2^v(x_2) - \phi_2^a(x_2)) \\
& \times \phi_3^T(x_3) - 2r_3(1-x_2+x_3)(\phi_2^v(x_2)\phi_3^v(x_3) - \phi_2^a(x_2)\phi_3^a(x_3))] h_{nfe}^c(x_1, x_2, x_3, b_1, b_2) \\
& \times E_{nfe}(t_c) + x_2(\phi_2^v(x_2) - \phi_2^a(x_2))\phi_3^T(x_3) E_{nfe}(t_d) h_{nfe}^d(x_1, x_2, x_3, b_1, b_2) \} , \quad (44)
\end{aligned}$$

$$\begin{aligned}
M_{nfe}^{P_2,T} = & \frac{32\sqrt{6}}{3}\pi C_F m_B^2 \int_0^1 dx_1 dx_2 dx_3 \int_0^\infty b_1 db_1 b_2 db_2 \phi_B(x_1, b_1) r_2 \{ [(1-x_2)(\phi_2^v(x_2) - \phi_2^a(x_2)) \\
& \times \phi_3^T(x_3) - 2r_3(1-x_2+x_3)(\phi_2^v(x_2)\phi_3^a(x_3) - \phi_2^a(x_2)\phi_3^v(x_3))] h_{nfe}^c(x_1, x_2, x_3, b_1, b_2) \\
& \times E_{nfe}(t_c) + x_2(\phi_2^v(x_2) - \phi_2^a(x_2))\phi_3^T(x_3) E_{nfe}(t_d) h_{nfe}^d(x_1, x_2, x_3, b_1, b_2) \} , \quad (45)
\end{aligned}$$

For the non-factorizable annihilation(nfa) diagrams 1(e) and 1(f), we have

$$\begin{aligned}
M_{nfa}^L = & -\frac{16\sqrt{6}}{3}\pi C_F m_B^2 \int_0^1 dx_1 dx_2 dx_3 \int_0^\infty b_1 db_1 b_2 db_2 \phi_B(x_1, b_1) \{ [(1-x_3)\phi_2(x_2)\phi_3(x_3) \\
& + r_2 r_3 ((1+x_2-x_3)(\phi_2^s(x_2)\phi_3^s(x_3) - \phi_2^t(x_2)\phi_3^t(x_3)) - (1-x_2-x_3)(\phi_2^s(x_2)\phi_3^t(x_3) \\
& - \phi_2^t(x_2)\phi_3^s(x_3))] E_{nfa}(t_e) h_{nfa}^e(x_1, x_2, x_3, b_1, b_2) - [x_2\phi_2(x_2)\phi_3(x_3) + 2r_2 r_3 (\phi_2^t(x_2) \\
& \times \phi_3^t(x_3) + \phi_2^s(x_2)\phi_3^s(x_3)) - r_2 r_3 (1+x_2-x_3)(\phi_2^t(x_2)\phi_3^t(x_3) - \phi_2^s(x_2)\phi_3^s(x_3)) + r_2 r_3 \\
& \times (1-x_2-x_3)(\phi_2^s(x_2)\phi_3^t(x_3) - \phi_2^t(x_2)\phi_3^s(x_3))] E_{nfa}(t_f) h_{nfa}^f(x_1, x_2, x_3, b_1, b_2) \} , \quad (46)
\end{aligned}$$

$$\begin{aligned}
M_{nfa}^N = & \frac{32\sqrt{6}}{3}\pi C_F m_B^2 \int_0^1 dx_1 dx_2 dx_3 \int_0^\infty b_1 db_1 b_2 db_2 \phi_B(x_1, b_1) r_2 r_3 \\
& \times [\phi_2^v(x_2)\phi_3^v(x_3) + \phi_2^a(x_2)\phi_3^a(x_3)] E_{nfa}(t_f) h_{nfa}^f(x_1, x_2, x_3, b_1, b_2) , \quad (47)
\end{aligned}$$

$$\begin{aligned}
M_{nfa}^T = & \frac{64\sqrt{6}}{3}\pi C_F m_B^2 \int_0^1 dx_1 dx_2 dx_3 \int_0^\infty b_1 db_1 b_2 db_2 \phi_B(x_1, b_1) r_2 r_3 \\
& \times [\phi_2^v(x_2)\phi_3^a(x_3) + \phi_2^a(x_2)\phi_3^v(x_3)] E_{nfa}(t_f) h_{nfa}^f(x_1, x_2, x_3, b_1, b_2) . \quad (48)
\end{aligned}$$

$$\begin{aligned}
M_{nfa}^{P_1,L} = & -\frac{16\sqrt{6}}{3}\pi C_F m_B^2 \int_0^1 dx_1 dx_2 dx_3 \int_0^\infty b_1 db_1 b_2 db_2 \phi_B(x_1, b_1) \{ [r_3(1-x_3)(\phi_3^s(x_3) - \phi_3^t(x_3)) \\
& \times \phi_2(x_2) + r_2 x_2(\phi_2^t(x_2) + \phi_2^s(x_2))\phi_3(x_3)] E_{nfa}(t_e) h_{nfa}^e(x_1, x_2, x_3, b_1, b_2) - [r_2(2-x_2)\phi_3(x_3) \\
& \times (\phi_2^t(x_2) + \phi_2^s(x_2)) - r_3(1+x_3)\phi_2(x_2)(\phi_3^s(x_3) - \phi_3^t(x_3))] E_{nfa}(t_f) h_{nfa}^f(x_1, x_2, x_3, b_1, b_2) \} , \quad (49)
\end{aligned}$$

$$\begin{aligned}
M_{nfa}^{P_1,N} = & -\frac{16\sqrt{6}}{3}\pi C_F m_B^2 \int_0^1 dx_1 dx_2 dx_3 \int_0^\infty b_1 db_1 b_2 db_2 \phi_B(x_1, b_1) \{ [r_2 x_2(\phi_2^v(x_2) + \phi_2^a(x_2))\phi_3^T(x_3) \\
& - r_3(1-x_3)\phi_2^T(x_2)(\phi_3^a(x_3) - \phi_3^v(x_3))] E_{nfa}(t_e) h_{nfa}^e(x_1, x_2, x_3, b_1, b_2) + [r_2(2-x_2)\phi_3^T(x_3) \\
& \times (\phi_2^v(x_2) + \phi_2^a(x_2)) - r_3(1+x_3)\phi_2^T(x_2)(\phi_3^a(x_3) - \phi_3^v(x_3))] E_{nfa}(t_f) h_{nfa}^f(x_1, x_2, x_3, b_1, b_2) \} , \quad (50)
\end{aligned}$$

$$M_{nfa}^{P_1,T} = 2M_{nfa}^{P_1,N} , \quad (51)$$

For the factorizable annihilation(fa) diagrams 1(g) and 1(h), the contributions are

$$\begin{aligned}
F_{fa}^L = & -8\pi C_F m_B^2 \int_0^1 dx_2 dx_3 \int_0^\infty b_2 db_2 b_3 db_3 \{ [x_2\phi_2(x_2)\phi_3(x_3) + 2r_3 r_3 \phi_3^s(x_3)((1+x_2)\phi_2^s(x_2) \\
& - (1-x_2)\phi_2^t(x_2))] E_{fa}(t_g) h_{fa}(x_2, 1-x_3, b_2, b_3) - [(1-x_3)\phi_2(x_2)\phi_3(x_3) + 2r_2 r_3 \phi_2^s(x_2) \\
& \times (x_3\phi_3^t(x_3) + (2-x_3)\phi_3^s(x_3))] E_{fa}(t_h) h_{fa}(1-x_3, x_2, b_3, b_2) \} , \quad (52)
\end{aligned}$$

$$\begin{aligned}
F_{fa}^N = & -8\pi C_F m_B^2 \int_0^1 dx_2 dx_3 \int_0^\infty b_2 db_2 b_3 db_3 r_2 r_3 \{ E_{fa}(t_g) [(1+x_2)(\phi_2^v(x_2)\phi_3^v(x_3) + \phi_2^a(x_2)\phi_3^a(x_3)) \\
& - (1-x_2)(\phi_2^v(x_2)\phi_3^a(x_3) + \phi_2^a(x_2)\phi_3^v(x_3))] h_{fa}(x_2, 1-x_3, b_2, b_3) - [(2-x_3)(\phi_2^v(x_2)\phi_3^v(x_3) \\
& + \phi_2^a(x_2)\phi_3^a(x_3)) + x_3(\phi_2^v(x_2)\phi_3^a(x_3) + \phi_2^a(x_2)\phi_3^v(x_3))] E_{fa}(t_h) h_{fa}(1-x_3, x_2, b_3, b_2) \} , \quad (53)
\end{aligned}$$

$$\begin{aligned}
F_{fa}^T = & -16\pi C_F m_B^2 \int_0^1 dx_2 dx_3 \int_0^\infty b_2 db_2 b_3 db_3 r_2 r_3 \{ E_{fa}(t_g) [(1+x_2)(\phi_2^v(x_2)\phi_3^a(x_3) + \phi_2^a(x_2)\phi_3^v(x_3)) \\
& - (1-x_2)(\phi_2^v(x_2)\phi_3^v(x_3) + \phi_2^a(x_2)\phi_3^a(x_3))] h_{fa}(x_2, 1-x_3, b_2, b_3) + [x_3(\phi_2^v(x_2)\phi_3^v(x_3) \\
& + \phi_2^a(x_2)\phi_3^a(x_3)) + (2-x_3)(\phi_2^v(x_2)\phi_3^a(x_3) + \phi_2^a(x_2)\phi_3^v(x_3))] E_{fa}(t_h) h_{fa}(1-x_3, x_2, b_3, b_2) \} ; \quad (54)
\end{aligned}$$

$$\begin{aligned}
F_{fa}^{P_2, L} = & -16\pi C_F m_B^2 \int_0^1 dx_2 dx_3 \int_0^\infty b_2 db_2 b_3 db_3 \{ [2r_3 \phi_2(x_2)\phi_3^s(x_3) - r_2 x_2(\phi_2^t(x_2) - \phi_2^s(x_2)) \\
& \times \phi_3(x_3)] h_{fa}(x_2, 1-x_3, b_2, b_3) E_{fa}(t_g) + [2r_2 \phi_2^s(x_2)\phi_3(x_3) + r_3(1-x_3)\phi_2(x_2) \\
& \times (\phi_3^t(x_3) + \phi_3^s(x_3))] E_{fa}(t_h) h_{fa}(1-x_3, x_2, b_3, b_2) \} , \quad (55)
\end{aligned}$$

$$\begin{aligned}
F_{fa}^{P_2, N} = & -16\pi C_F m_B^2 \int_0^1 dx_2 dx_3 \int_0^\infty b_2 db_2 b_3 db_3 \{ r_3 \phi_2^T(x_2)(\phi_3^a(x_3) - \phi_3^v(x_3)) h_{fa}(x_2, 1-x_3, b_2, b_3) \\
& \times E_{fa}(t_g) + r_2(\phi_2^v(x_2) + \phi_2^a(x_2))\phi_3^T(x_3) E_{fa}(t_h) h_{fa}(1-x_3, x_2, b_3, b_2) \} , \quad (56)
\end{aligned}$$

$$F_{fa}^{P_2, T} = 2F_{fa}^{P_2, N}; \quad (57)$$

Before we put the things together to write down the decay amplitudes for the considered $B \rightarrow \phi K_1$ modes, it is essential to give a brief discussion about the " $K_1(1270) - K_1(1400)$ " mixing. The physical mass eigenstates $K_1(1270)$ and $K_1(1400)$ are believed to be the mixtures of the $K_{1A}(^3P_1)$ and $K_{1B}(^1P_1)$ states with the mixing angle θ_{K_1} due to the mass difference of the strange and non-strange light quarks. Following the common convention, their relations can be written as [40]

$$\begin{pmatrix} |K_1(1270)\rangle \\ |K_1(1400)\rangle \end{pmatrix} = \begin{pmatrix} \sin \theta_{K_1} & \cos \theta_{K_1} \\ \cos \theta_{K_1} & -\sin \theta_{K_1} \end{pmatrix} \begin{pmatrix} |K_{1A}\rangle \\ |K_{1B}\rangle \end{pmatrix}, \quad (58)$$

There exist several estimations on the mixing angle θ_{K_1} in the literature [43–48]. Various phenomenological studies indicate that the $K_{1A} - K_{1B}$ mixing angle θ_{K_1} is around either 33° or 58° but with a twofold ambiguity. The sign ambiguity for θ_{K_1} is due to the fact that one can add arbitrary phases to $|K_{1A}\rangle$ and $|K_{1B}\rangle$. As discussed in Ref. [47] and many early publications, the sign ambiguity of θ_{K_1} can be removed by fixing the relative sign of the decay constants of $|K_{1A}\rangle$ and $|K_{1B}\rangle$. We shall choose the convention of decay constants in such a way that θ_{K_1} is always positive. It is noted that the sign of the mixing angle θ_{K_1} is positive for the mixing of particle states K_{1A} and K_{1B} in this work, which corresponds to the negative sign of θ_{K_1} between the mixing of antiparticle states \bar{K}_{1A} and \bar{K}_{1B} in the literature [46]. The underlying reason is that, as discussed in Ref. [49], the spin-orbit portion $\langle H_{q\bar{q}}^{SO} \rangle$ in the constituent quark model Hamiltonian causes the mixing between $K_{1A}(^3P_1)$ and $K_{1B}(^1P_1)$ states, changes the sign when the antiquark instead of the quark is the heavier strange, then further leads to a mixing angle of opposite sign when the $^3P_1 - ^1P_1$ Hamiltonian is diagonalized. In other words, if we have a angle of -33° for the mixing of antiparticles $K_1(1270)^-$ and $K_1(1400)^-$, we must use $+33^\circ$ for that of the particles $K_1(1270)^+$ and $K_1(1400)^+$. For the value of mixing angle θ_{K_1} , we shall adopt both 33° and 58° in the numerical evaluations, which is because almost no any precise measurements on θ_{K_1} exist to date and one can identify the more favored value of the mixing angle in the relevant B meson decays, though Refs. [1, 46, 47] suggested that the smaller angle $\theta_{K_1} \sim 33^\circ$ is much more favored than 58° .

Thus, by combining various contributions from different diagrams as presented in Eqs. (33)-(57) and the mixing pattern in Eq. (58), the total decay amplitudes for the penguin dominated $B \rightarrow \phi K_1(1270)$ can be written as

$$\begin{aligned}
\mathcal{M}_h(B^+ \rightarrow \phi K_1(1270)^+) &= A_h(B^+ \rightarrow \phi K_{1A}^+) \sin\theta_{K_1} + A_h(B^+ \rightarrow \phi K_{1B}^+) \cos\theta_{K_1} \\
&= -\lambda_t f_\phi \left(a_3 + a_4 + a_5 - \frac{1}{2}(a_7 + a_9 + a_{10}) \right) (F_{fe;K_{1A}}^h \sin\theta_{K_1} + F_{fe;K_{1B}}^h \cos\theta_{K_1}) \\
&\quad - \lambda_t \left\{ (M_{nfe;K_{1A}}^h \sin\theta_{K_1} + M_{nfe;K_{1B}}^h \cos\theta_{K_1}) (C_3 + C_4 - \frac{1}{2}(C_9 + C_{10})) \right. \\
&\quad + (C_5 - \frac{1}{2}C_7) (M_{nfe;K_{1A}}^{P_1;h} \sin\theta_{K_1} + M_{nfe;K_{1B}}^{P_1;h} \cos\theta_{K_1}) + (C_6 - \frac{1}{2}C_8) (M_{nfe;K_{1A}}^{P_2;h} \\
&\quad \cdot \sin\theta_{K_1} + \cos\theta_{K_1} M_{nfe;K_{1B}}^{P_2;h}) \left. \right\} + \lambda_u C_1 (M_{nfa;K_{1A}}^h \sin\theta_{K_1} + M_{nfa;K_{1B}}^h \cos\theta_{K_1}) \\
&\quad - \lambda_t \left\{ (C_3 + C_9) (M_{nfa;K_{1A}}^h \sin\theta_{K_1} + M_{nfa;K_{1B}}^h \cos\theta_{K_1}) + (C_5 + C_7) \right. \\
&\quad \cdot (M_{nfa;K_{1A}}^{P_1;h} \sin\theta_{K_1} + M_{nfa;K_{1B}}^{P_1;h} \cos\theta_{K_1}) \left. \right\} + \lambda_u a_1 (F_{fa;K_{1A}}^h \sin\theta_{K_1} + F_{fa;K_{1B}}^h \\
&\quad \cdot \cos\theta_{K_1}) f_B - \lambda_t \left\{ (a_4 + a_{10}) (F_{fa;K_{1A}}^h \sin\theta_{K_1} + F_{fa;K_{1B}}^h \cos\theta_{K_1}) + (a_6 + a_8) \right. \\
&\quad \cdot (F_{fa;K_{1A}}^{P_2;h} \sin\theta_{K_1} + F_{fa;K_{1B}}^{P_2;h} \cos\theta_{K_1}) \left. \right\} f_B; \tag{59}
\end{aligned}$$

$$\begin{aligned}
\mathcal{M}_h(B^0 \rightarrow \phi K_1(1270)^0) &= A_h(B^0 \rightarrow \phi K_{1A}^0) \sin\theta_{K_1} + A_h(B^0 \rightarrow \phi K_{1B}^0) \cos\theta_{K_1} \\
&= -\lambda_t f_\phi \left(a_3 + a_4 + a_5 - \frac{1}{2}(a_7 + a_9 + a_{10}) \right) (F_{fe;K_{1A}}^h \sin\theta_{K_1} + F_{fe;K_{1B}}^h \cos\theta_{K_1}) \\
&\quad - \lambda_t \left\{ (M_{nfe;K_{1A}}^h \sin\theta_{K_1} + M_{nfe;K_{1B}}^h \cos\theta_{K_1}) (C_3 + C_4 - \frac{1}{2}(C_9 + C_{10})) \right. \\
&\quad + (C_5 - \frac{1}{2}C_7) (M_{nfe;K_{1A}}^{P_1;h} \sin\theta_{K_1} + M_{nfe;K_{1B}}^{P_1;h} \cos\theta_{K_1}) + (C_6 - \frac{1}{2}C_8) (M_{nfe;K_{1A}}^{P_2;h} \\
&\quad \cdot \sin\theta_{K_1} + \cos\theta_{K_1} M_{nfe;K_{1B}}^{P_2;h}) \left. \right\} - \lambda_t \left\{ (C_3 - \frac{1}{2}C_9) (M_{nfa;K_{1A}}^h \sin\theta_{K_1} + M_{nfa;K_{1B}}^h \cos\theta_{K_1}) \right. \\
&\quad \cdot \cos\theta_{K_1}) + (C_5 - \frac{1}{2}C_7) (M_{nfa;K_{1A}}^{P_1;h} \sin\theta_{K_1} + M_{nfa;K_{1B}}^{P_1;h} \cos\theta_{K_1}) \left. \right\} - \lambda_t f_B \left\{ (a_4 - \frac{1}{2}a_{10}) \right. \\
&\quad \cdot (F_{fa;K_{1A}}^h \sin\theta_{K_1} + F_{fa;K_{1B}}^h \cos\theta_{K_1}) + (a_6 - \frac{1}{2}a_8) (F_{fa;K_{1A}}^{P_2;h} \sin\theta_{K_1} + F_{fa;K_{1B}}^{P_2;h} \cos\theta_{K_1}) \left. \right\} \tag{60}
\end{aligned}$$

where $\lambda_u = V_{ub}^* V_{us}$, $\lambda_t = V_{tb}^* V_{ts}$ and \mathcal{M}_h in the above equations denotes the different helicity amplitudes \mathcal{M}_L , \mathcal{M}_N , and \mathcal{M}_T , respectively. And a_i is the standard combination of the Wilson coefficients C_i defined as follows:

$$a_1 = C_2 + \frac{C_1}{3}; \quad a_i = C_i + C_{i\pm 1}/3, \quad i = 3 - 10. \tag{61}$$

where $C_2 \sim 1$ is the largest one among all Wilson coefficients and the upper (lower) sign applies, when i is odd (even). When we make the replacements with $\sin\theta_{K_1} \rightarrow \cos\theta_{K_1}$, $\cos\theta_{K_1} \rightarrow -\sin\theta_{K_1}$ in Eqs.(59) and (60), respectively, the total decay amplitudes for the $B \rightarrow \phi K_1(1400)$ decays can be obtained straightforwardly.

III. NUMERICAL RESULTS AND DISCUSSIONS

In this section, we will present the pQCD predictions on the CP-averaged branching ratios, the polarization fractions, the relative phases and the CP-violating asymmetries for those four $B \rightarrow \phi K_1$ decay modes. In numerical calculations, central values of the input parameters will be used implicitly unless otherwise stated. The relevant QCD scale (GeV), masses (GeV), and B meson lifetime(ps) are the following [15–17, 38, 40]

$$\begin{aligned}
\Lambda_{\overline{\text{MS}}}^{(f=4)} &= 0.250, \quad m_W = 80.41, \quad m_B = 5.2794, \quad m_b = 4.8, \quad m_\phi = 1.02; \\
f_{K_{1A}} &= 0.250, \quad f_{K_{1B}} = 0.190, \quad m_{K_{1A}} = 1.32, \quad m_{K_{1B}} = 1.34, \\
\tau_{B^+} &= 1.641, \quad \tau_{B^0} = 1.519. \tag{62}
\end{aligned}$$

For the CKM matrix elements, we adopt the Wolfenstein parametrization and the updated parameters $A = 0.811$, $\lambda = 0.22535$, $\bar{\rho} = 0.131^{+0.026}_{-0.013}$, and $\bar{\eta} = 0.345^{+0.013}_{-0.014}$ [40].

A. CP-averaged branching ratios

For the considered $B \rightarrow \phi K_1$ decays, the decay rate can be written as

$$\Gamma = \frac{G_F^2 |\mathbf{P}_c|}{16\pi m_B^2} \sum_{\sigma=L,T} \mathcal{M}^{(\sigma)\dagger} \mathcal{M}^{(\sigma)} \quad (63)$$

where $|\mathbf{P}_c| \equiv |\mathbf{P}_{2z}| = |\mathbf{P}_{3z}|$ is the momentum of either of the outgoing axial-vector meson or vector meson and $\mathcal{M}^{(\sigma)}$ can be found in Eqs. (59-60). Using the decay amplitudes obtained in last section, it is straightforward to calculate the CP-averaged branching ratios with uncertainties for the considered decays in the pQCD approach. The numerical results of the physical

TABLE I. Theoretical predictions on physical quantities of $B^+ \rightarrow \phi K_1(1270)^+$ decay obtained in the pQCD approach with the mixing angle $\theta_{K_1} \sim 33^\circ$ and 58° , respectively. For comparison, we also quote the available experimental measurements [2] and the estimations in the framework of QCD factorization [9].

Decay Mode		$B^+ \rightarrow \phi K_1(1270)^+$				
Parameter	Definition	pQCD ($\theta_{K_1} \sim 33^\circ$)	QCDF ($\theta_{K_1} \sim 37^\circ$)	pQCD ($\theta_{K_1} \sim 58^\circ$)	QCDF ($\theta_{K_1} \sim 58^\circ$)	Experiment
BR(10^{-6})	$\Gamma/\Gamma_{\text{total}}$	$5.4^{+0.9+0.5+3.3+2.1}_{-0.5-0.5-2.3-1.2}$	$3.8^{+1.9+5.1}_{-1.5-3.1}$	$9.2^{+0.2+1.3+4.4+2.5}_{-0.2-1.2-3.4-1.9}$	$3.4^{+2.2+5.5}_{-1.5-2.8}$	$6.1 \pm 1.6 \pm 1.1$
f_L	$ A_L ^2$	$0.47^{+0.11+0.08+0.28+0.01}_{-0.09-0.06-0.30-0.00}$	$0.67^{+0.33}_{-0.64}$	$0.11^{+0.00+0.00+0.11+0.01}_{-0.01-0.02-0.07-0.01}$	$0.31^{+0.69}_{-0.37}$	$0.46^{+0.12+0.06}_{-0.13-0.07}$
$f_{ }$	$ A_{ } ^2$	$0.30^{+0.06+0.03+0.17+0.00}_{-0.06-0.03-0.19-0.00}$	—	$0.45^{+0.01+0.00+0.06+0.00}_{-0.01-0.02-0.11-0.00}$	—	—
f_\perp	$ A_\perp ^2$	$0.22^{+0.04+0.05+0.17+0.00}_{-0.04-0.03-0.14-0.00}$	—	$0.45^{+0.01+0.00+0.05+0.01}_{-0.01-0.01-0.08-0.02}$	—	—
$\phi_{ }(\text{rad})$	$\arg \frac{A_{ }}{A_L}$	$2.2^{+0.1+0.0+0.3+0.1}_{-0.1-0.1-0.3-0.1}$	—	$3.3^{+0.0+0.1+0.6+0.0}_{-0.0-0.1-0.9-0.1}$	—	—
$\phi_\perp(\text{rad})$	$\arg \frac{A_\perp}{A_L}$	$4.4^{+0.0+0.1+0.2+0.0}_{-1.4-0.1-2.4-1.4}$	—	$2.6^{+0.0+0.1+0.7+0.0}_{-0.0-0.1-1.0-0.0}$	—	—
$\mathcal{A}_{CP}^{\text{dir}}(10^{-2})$	$\frac{\Gamma - \bar{\Gamma}}{\Gamma + \bar{\Gamma}}$	$-0.7^{+0.5+0.5+3.3+1.2}_{-0.3-0.4-2.6-1.3}$	—	$-1.3^{+0.0+0.3+0.9+0.5}_{-0.1-0.2-0.5-0.6}$	—	$-15 \pm 19 \pm 5$
$\mathcal{A}_{CP}^{\text{dir}}(L)$	$\frac{f_L - \bar{f}_L}{f_L + \bar{f}_L}$	$0.04^{+0.09}_{-0.07}$	—	$0.16^{+0.08}_{-0.10}$	—	—
$\mathcal{A}_{CP}^{\text{dir}}()$	$\frac{f_{ } - \bar{f}_{ }}{f_{ } + \bar{f}_{ }}$	$-0.33^{+0.12}_{-0.14}$	—	$-0.29^{+0.09}_{-0.08}$	—	—
$\mathcal{A}_{CP}^{\text{dir}}(\perp)$	$\frac{f_\perp - \bar{f}_\perp}{f_\perp + \bar{f}_\perp}$	$0.33^{+0.11}_{-0.09}$	—	$0.22^{+0.05}_{-0.05}$	—	—

quantities are presented in Tables I-IV, in which the major errors are induced by the uncertainties of the shape parameter $\omega_b = 0.40 \pm 0.04$ GeV for the B meson wave function, of the vector ϕ meson decay constants $f_\phi = 0.231 \pm 0.004$ GeV and $f_\phi^T = 0.200 \pm 0.010$ GeV and the axial-vector K_{1A} and K_{1B} states decay constants $f_{K_{1A}} = 0.250 \pm 0.013$ GeV and $f_{K_{1B}} = 0.190 \pm 0.010$ GeV, and of the Gegenbauer moments $a_i^{A,B}$ ($i = 0, 1, 2$) for the axial-vector K_{1A} and K_{1B} states and a_2 for the vector ϕ meson in both longitudinal and transverse polarizations, respectively. Moreover, in this work, as displayed in the above mentioned Tables, the higher order contributions are also simply investigated by exploring the variation of the hard scale t_{max} , i.e., from $0.8t$ to $1.2t$ (not changing $1/b_i$, $i = 1, 2, 3$), in the hard kernel, which have been counted into one of the source of theoretical uncertainties (See the last term of errors in the related Tables). Note that the variation of the CKM parameters has tiny or almost no effects to the physical observables of these $B \rightarrow \phi K_1$ decays in the pQCD approach and thus have been neglected in the relevant numerical results.

Based on the theoretical branching ratios given at leading order in the pQCD approach, some phenomenological remarks on the $B \rightarrow \phi K_1$ decays are in order:

- From Table I, one can easily find that the CP-averaged branching ratios of $B^+ \rightarrow \phi K_1(1270)^+$ decay are

$$Br(B^+ \rightarrow \phi K_1(1270)^+)_{\text{pQCD}} = \begin{cases} 5.4^{+4.0}_{-2.7} \times 10^{-6} & \theta_{K_1} \sim 33^\circ \\ 9.2^{+5.2}_{-4.1} \times 10^{-6} & \theta_{K_1} \sim 58^\circ \end{cases}, \quad (64)$$

where various errors arising from the input parameters have been added in quadrature. It is observed that the former prediction with the smaller angle 33° is more consistent with the available measurement [2],

$$Br(B^\pm \rightarrow \phi K_1(1270)^\pm)_{\text{Exp.}} = (6.1 \pm 1.9) \times 10^{-6}, \quad (65)$$

TABLE II. Same as Table I but of $B^+ \rightarrow \phi K_1(1400)^+$ decay.

Decay Mode		$B^+ \rightarrow \phi K_1(1400)^+$				
Parameter	Definition	pQCD ($\theta_{K_1} \sim 33^\circ$)	QCDF ($\theta_{K_1} \sim 37^\circ$)	pQCD ($\theta_{K_1} \sim 58^\circ$)	QCDF ($\theta_{K_1} \sim 58^\circ$)	Experiment
$Br(10^{-6})$	$\Gamma/\Gamma_{\text{total}}$	$25.1^{+8.5+2.1+10.7+4.4}_{-6.0-2.2-8.9-3.7}$	$11.1^{+8.5+41.1}_{-5.4-11.4}$	$21.4^{+9.3+2.0+7.9+3.9}_{-6.3-1.8-6.7-3.0}$	$11.3^{+7.5+40.2}_{-4.9-11.1}$	$< 3.2(0.3 \pm 1.6 \pm 0.7)(90\% \text{ C.L.})$
f_L	$ \mathcal{A}_L ^2$	$0.57^{+0.06+0.03+0.12+0.02}_{-0.06-0.02-0.11-0.02}$	$0.45^{+0.13}_{-0.09}$	$0.74^{+0.04+0.02+0.10+0.02}_{-0.04-0.02-0.09-0.00}$	$0.57^{+0.32}_{-0.22}$	—
$f_{ }$	$ \mathcal{A}_{ } ^2$	$0.20^{+0.03+0.01+0.07+0.01}_{-0.03-0.02-0.06-0.01}$	—	$0.12^{+0.02+0.00+0.06+0.00}_{-0.02-0.00-0.05-0.01}$	—	—
f_{\perp}	$ \mathcal{A}_{\perp} ^2$	$0.23^{+0.03+0.00+0.05+0.01}_{-0.03-0.02-0.05-0.01}$	—	$0.14^{+0.02+0.00+0.04+0.00}_{-0.02-0.02-0.05-0.01}$	—	—
$\phi_{ }(\text{rad})$	$\arg \frac{\mathcal{A}_{ }}{\mathcal{A}_L}$	$4.1^{+0.1+0.0+0.2+0.1}_{-0.1-0.0-0.2-0.0}$	—	$4.0^{+0.1+0.0+0.2+0.1}_{-0.1-0.0-0.3-0.0}$	—	—
$\phi_{\perp}(\text{rad})$	$\arg \frac{\mathcal{A}_{\perp}}{\mathcal{A}_L}$	$3.7^{+0.0+0.0+0.2+0.1}_{-0.0-0.0-0.2-0.1}$	—	$3.8^{+0.0+0.0+0.2+0.1}_{-0.0-0.0-0.2-0.1}$	—	—
$\mathcal{A}_{CP}^{\text{dir}}(10^{-2})$	$\frac{\Gamma-\bar{\Gamma}}{\Gamma+\bar{\Gamma}}$	$-1.5^{+0.3+0.1+1.1+0.3}_{-0.4-0.1-1.4-0.3}$	—	$-1.3^{+0.2+0.0+1.4+0.5}_{-0.4-0.2-1.6-0.5}$	—	—
$\mathcal{A}_{CP}^{\text{dir}}(L)$	$\frac{f_L-f_{\bar{L}}}{f_L+f_{\bar{L}}}$	$-0.01^{+0.02}_{-0.02}$	—	$-0.01^{+0.01}_{-0.04}$	—	—
$\mathcal{A}_{CP}^{\text{dir}}()$	$\frac{f_{ }-f_{\bar{ }}}{f_{ }+f_{\bar{ }}}$	$-0.17^{+0.05}_{-0.03}$	—	$-0.08^{+0.05}_{-0.06}$	—	—
$\mathcal{A}_{CP}^{\text{dir}}(\perp)$	$\frac{f_{\perp}-f_{\bar{\perp}}}{f_{\perp}+f_{\bar{\perp}}}$	$0.11^{+0.02}_{-0.04}$	—	$0.05^{+0.03}_{-0.06}$	—	—

where the systematic and statistical errors have also been added in quadrature, although the latter prediction basically agrees with the theoretical values obtained in the framework of QCD factorization and the preliminary data reported by BABAR Collaboration within large errors.

- According to Table II, the CP-averaged branching ratios of $B^+ \rightarrow \phi K_1(1400)^+$ decay with two different mixing angles can be read as

$$Br(B^+ \rightarrow \phi K_1(1400)^+)_{\text{pQCD}} = \begin{cases} 25.1^{+14.5}_{-11.6} \times 10^{-6} & \theta_{K_1} \sim 33^\circ \\ 21.4^{+13.0}_{-9.8} \times 10^{-6} & \theta_{K_1} \sim 58^\circ \end{cases}, \quad (66)$$

Here, we have added all the errors in quadrature. Our theoretical predictions are in agreement with that derived in the QCDF approach within large errors and also with the preliminary upper limit [2]

$$Br(B^\pm \rightarrow \phi K_1(1400)^\pm)_{\text{Exp.}} < 3.2(0.3 \pm 1.6 \pm 0.7) \times 10^{-6}, \quad (67)$$

in 2σ errors roughly. But, it looks that, unfortunately, the central values significantly exceed the upper limit placed by only BABAR Collaboration. It will be very interesting and probably a challenge for the theorists to further understand the QCD dynamics of these two strange axial-vector mesons and the mixing between K_{1A} and K_{1B} states in depth once the experiments at LHC and/or Super-B confirm the aforementioned much small upper limits of $Br(B^+ \rightarrow \phi K_1(1400)^+)$ in the near future.

- As can be seen in Tables III and IV, the CP-averaged branching ratios of $B^0 \rightarrow \phi K_1^0$ decays with two different mixing angles are also predicted in the pQCD approach,

$$Br(B^0 \rightarrow \phi K_1(1270)^0)_{\text{pQCD}} = \begin{cases} 5.1^{+3.5}_{-2.7} \times 10^{-6} & \theta_{K_1} \sim 33^\circ \\ 9.2^{+5.5}_{-4.0} \times 10^{-6} & \theta_{K_1} \sim 58^\circ \end{cases}, \quad (68)$$

$$Br(B^0 \rightarrow \phi K_1(1400)^0)_{\text{pQCD}} = \begin{cases} 22.5^{+12.8}_{-10.3} \times 10^{-6} & \theta_{K_1} \sim 33^\circ \\ 18.5^{+11.3}_{-8.8} \times 10^{-6} & \theta_{K_1} \sim 58^\circ \end{cases}. \quad (69)$$

which are consistent with the predictions in the QCDF approach within large theoretical errors and will be tested in the running LHC and forthcoming Super-B experiments.

- As discussed in Refs. [9, 38], the behavior of the axial-vector 3P_1 states is similar to that of the vector mesons, which will consequently result in the branching ratio of $B \rightarrow \phi K_{1A}$ analogous to that of $B \rightarrow \phi K^*$ decays in the pQCD approach. However, from Tables I-IV, it can be clearly observed that the predicted branching ratios of $B \rightarrow \phi K_1(1270)(B \rightarrow \phi K_1(1400))$ decays in the pQCD approach are smaller(larger) than those of $B \rightarrow \phi K^*$ decays [42], which imply the destructive(constructive) effects between $B \rightarrow \phi K_{1A}$ and $B \rightarrow \phi K_{1B}$ decay amplitudes to $B \rightarrow \phi K_1(1270)(B \rightarrow \phi K_1(1400))$ decays. In order to clarify this point more clearly, we present the decay amplitudes of the $B^+ \rightarrow \phi K_{1A}^+$ and $B^+ \rightarrow \phi K_{1B}^+$ decays numerically for every topology with three polarizations, which can be seen in Table V.

TABLE III. Same as Table I but of $B^0 \rightarrow \phi K_1(1270)^0$ decay.

Decay Mode		$B^0 \rightarrow \phi K_1(1270)^0$				
Parameter	Definition	pQCD ($\theta_{K_1} \sim 33^\circ$)	QCDF ($\theta_{K_1} \sim 37^\circ$)	pQCD ($\theta_{K_1} \sim 58^\circ$)	QCDF ($\theta_{K_1} \sim 58^\circ$)	Experiment
$BR(10^{-6})$	$\Gamma/\Gamma_{\text{total}}$	$5.1^{+0.7+0.4+2.9+1.8}_{-0.5-0.5-2.3-1.2}$	$3.6^{+1.7+4.8}_{-1.3-2.9}$	$9.2^{+0.2+1.3+4.7+2.5}_{-0.1-1.2-3.4-1.8}$	$3.2^{+2.1+5.2}_{-1.4-2.7}$	—
f_L	$ \mathcal{A}_L ^2$	$0.42^{+0.11+0.06+0.30+0.01}_{-0.09-0.06-0.28-0.00}$	$0.67^{+0.33}_{-0.64}$	$0.11^{+0.00+0.02+0.13+0.01}_{-0.00-0.01-0.06-0.00}$	$0.31^{+0.69}_{-0.31}$	—
$f_{ }$	$ \mathcal{A}_{ } ^2$	$0.35^{+0.05+0.02+0.14+0.00}_{-0.07-0.04-0.20-0.01}$	—	$0.45^{+0.01+0.00+0.07+0.01}_{-0.01-0.00-0.11-0.00}$	—	—
f_\perp	$ \mathcal{A}_\perp ^2$	$0.24^{+0.03+0.03+0.13+0.00}_{-0.05-0.05-0.17-0.01}$	—	$0.44^{+0.01+0.00+0.05+0.01}_{-0.01-0.01-0.07-0.02}$	—	—
$\phi_{ }(\text{rad})$	$\arg \frac{\mathcal{A}_{ }}{\mathcal{A}_L}$	$2.3^{+0.1+0.1+0.4+0.1}_{-0.1-0.1-0.3-0.1}$	—	$3.4^{+0.0+0.1+0.5+0.0}_{-0.0-0.1-0.8-0.1}$	—	—
$\phi_\perp(\text{rad})$	$\arg \frac{\mathcal{A}_\perp}{\mathcal{A}_L}$	$4.4^{+0.2+0.1+0.5+0.2}_{-0.2-0.1-0.4-0.2}$	—	$2.7^{+0.0+0.1+0.6+0.0}_{-0.0-0.1-0.9-0.0}$	—	—
$\mathcal{A}_{CP}^{\text{dir}}(10^{-2})$	$\frac{\Gamma-\bar{\Gamma}}{\Gamma+\bar{\Gamma}}$	0.0	—	0.0	—	—
$\mathcal{A}_{CP}^{\text{dir}}(L)$	$\frac{f_L - \bar{f}_L}{f_L + \bar{f}_L}$	0.0	—	0.0	—	—
$\mathcal{A}_{CP}^{\text{dir}}()$	$\frac{f_{ } - \bar{f}_{ }}{f_{ } + \bar{f}_{ }}$	0.0	—	0.0	—	—
$\mathcal{A}_{CP}^{\text{dir}}(\perp)$	$\frac{f_\perp - \bar{f}_\perp}{f_\perp + \bar{f}_\perp}$	0.0	—	0.0	—	—

- As mentioned in the Introduction, up to now, the penguin-dominated $B \rightarrow \phi K_1$ decays have been investigated with different approaches/methods [9–11]. With the form factors of $B \rightarrow K_1$ transitions calculated in the improved Isgur-Scora-Grinstein-Wise quark model, the authors got the branching ratios of $B \rightarrow \phi K_1(1270)$ and $B \rightarrow \phi K_1(1400)$ decays with two different mixing angles 32° and 58° [10] in the naive factorization approach. However, the results of the former modes are too small ($10^{-9} \sim 10^{-7}$) to be comparable with the available measurements and that for the latter ones are consistent with the preliminary upper limits. Those branching ratios indicate the destructive(constructive) interferences between $B \rightarrow \phi K_{1A}$ and $B \rightarrow \phi K_{1B}$. With the $B \rightarrow K_{1A}$ and $B \rightarrow K_{1B}$ form factors taken from light-front quark model and by neglecting the so-called “negligible” annihilation contributions, the authors obtained the $\mathcal{O}(10^{-5})$ and $\mathcal{O}(10^{-6})$ branching ratios in the generalized factorization approach for $B \rightarrow \phi K_1(1270)$ and $B \rightarrow \phi K_1(1400)$ decays, respectively, when the preferred effective color number N_c^{eff} is 2 or 3, which exhibit the constructive(destructive) contributions to $B \rightarrow \phi K_1(1270)$ ($B \rightarrow \phi K_1(1400)$) modes and the contrary decay pattern to that given in Ref. [10].
- Armed with the light-cone wave functions of axial-vector mesons in QCD sum rule method, Cheng and Yang studied the $B \rightarrow \phi K_1$ decays explicitly in the QCDF approach [9]. The predictions for the branching ratios of the considered $B \rightarrow \phi K_1$ decays in QCDF are also presented in Tables I–IV. It is necessary to point out that the evaluations on these $B \rightarrow \phi K_1$ decays in QCDF have used the weak annihilation parameters, which can be sizable and important on polarizations [11], inferred from the vector-vector $B \rightarrow \phi K^*$ decays. The QCDF predictions show the similar interferences between $B \rightarrow \phi K_{1A}$ and $B \rightarrow \phi K_{1B}$ to that shown in the pQCD approach, which is more apparent in both predictions with the smaller mixing angle 33° . Moreover, according to the CP-averaged branching ratios of $B \rightarrow \phi K_1$ decays, the QCDF results show the weak dependence of mixing angle, while the pQCD values exhibit the stronger(weaker) sensitivity to the mixing angle in $B \rightarrow \phi K_1(1270)$ ($B \rightarrow \phi K_1(1400)$) decays. The underlying reason is that with the increasing of the mixing angle θ_{K_1} , the significantly destructive interferences on longitudinal polarization and dramatically constructive effects (specifically, in the annihilation diagrams) on both transverse polarizations between $B \rightarrow \phi K_{1A}$ and $B \rightarrow \phi K_{1B}$ (See Table V) result in the large branching ratios but small longitudinal polarization fraction in $B \rightarrow \phi K_1(1270)$ decays.
- In view of the large theoretical errors from the hadronic parameters in the pQCD predictions, we define the interesting ratios as follows,

$$\frac{Br(B^+ \rightarrow \phi K_1(1270)^+)}{Br(B^+ \rightarrow \phi K_1(1400)^+)} = \begin{cases} 0.22^{+0.20}_{-0.15} & \theta_{K_1} \sim 33^\circ \\ 0.43^{+0.36}_{-0.27} & \theta_{K_1} \sim 58^\circ \end{cases}, \quad (70)$$

$$\frac{Br(B^0 \rightarrow \phi K_1(1270)^0)}{Br(B^0 \rightarrow \phi K_1(1400)^0)} = \begin{cases} 0.23^{+0.20}_{-0.16} & \theta_{K_1} \sim 33^\circ \\ 0.50^{+0.43}_{-0.32} & \theta_{K_1} \sim 58^\circ \end{cases}, \quad (71)$$

$$\frac{\tau_{B^0}}{\tau_{B^+}} \cdot \frac{Br(B^+ \rightarrow \phi K_1(1270)^+)}{Br(B^0 \rightarrow \phi K_1(1270)^0)} = \begin{cases} 0.98^{+0.99}_{-0.71} & \theta_{K_1} \sim 33^\circ \\ 0.93^{+0.76}_{-0.58} & \theta_{K_1} \sim 58^\circ \end{cases}, \quad (72)$$

TABLE IV. Same as Table I but of $B^0 \rightarrow \phi K_1(1400)^0$ decay.

Decay Mode		$B^0 \rightarrow \phi K_1(1400)^0$				
Parameter	Definition	pQCD ($\theta_{K_1} \sim 33^\circ$)	QCDF ($\theta_{K_1} \sim 37^\circ$)	pQCD ($\theta_{K_1} \sim 58^\circ$)	QCDF ($\theta_{K_1} \sim 58^\circ$)	Experiment
BR(10^{-6})	$\Gamma/\Gamma_{\text{total}}$	$22.5^{+7.7+2.0+9.2+4.0}_{-5.3-2.1-7.9-3.3}$	$10.4^{+7.9+38.3}_{-5.1-10.4}$	$18.5^{+8.2+1.8+6.7+3.4}_{-5.6-1.8-5.9-2.7}$	$10.7^{+7.1+37.7}_{-4.6-10.4}$	—
f_L	$ \mathcal{A}_L ^2$	$0.55^{+0.06+0.02+0.10+0.00}_{-0.07-0.03-0.13-0.00}$	$0.46^{+0.26}_{-0.02}$	$0.72^{+0.04+0.02+0.11+0.02}_{-0.05-0.02-0.10-0.01}$	$0.57^{+0.31}_{-0.22}$	—
$f_{ }$	$ \mathcal{A}_{ } ^2$	$0.21^{+0.03+0.01+0.06+0.00}_{-0.03-0.02-0.07-0.00}$	—	$0.12^{+0.03+0.02+0.07+0.01}_{-0.01-0.00-0.04-0.00}$	—	—
f_\perp	$ \mathcal{A}_\perp ^2$	$0.25^{+0.03+0.00+0.05+0.00}_{-0.04-0.02-0.06-0.01}$	—	$0.15^{+0.03+0.02+0.06+0.01}_{-0.02-0.00-0.04-0.01}$	—	—
$\phi_{ }$ (rad)	$\arg \frac{\mathcal{A}_{ }}{\mathcal{A}_L}$	$4.2^{+0.1+0.0+0.2+0.1}_{-0.1-0.0-0.2-0.0}$	—	$4.1^{+0.1+0.0+0.2+0.1}_{-0.1-0.0-0.3-0.0}$	—	—
ϕ_\perp (rad)	$\arg \frac{\mathcal{A}_\perp}{\mathcal{A}_L}$	$3.7^{+0.0+0.0+0.2+0.1}_{-0.0-0.0-0.2-0.1}$	—	$3.8^{+0.1+0.0+0.3+0.1}_{-0.0-0.0-0.3-0.1}$	—	—
$\mathcal{A}_{CP}^{\text{dir}}(10^{-2})$	$\frac{\Gamma-\bar{\Gamma}}{\Gamma+\bar{\Gamma}}$	0.0	—	0.0	—	—
$\mathcal{A}_{CP}^{\text{dir}}(L)$	$\frac{f_L-\bar{f}_L}{f_L+\bar{f}_L}$	0.0	—	0.0	—	—
$\mathcal{A}_{CP}^{\text{dir}}()$	$\frac{f_{ }-\bar{f}_{ }}{f_{ }+\bar{f}_{ }}$	0.0	—	0.0	—	—
$\mathcal{A}_{CP}^{\text{dir}}(\perp)$	$\frac{f_\perp-\bar{f}_\perp}{f_\perp+\bar{f}_\perp}$	0.0	—	0.0	—	—

$$\frac{\tau_{B^0}}{\tau_{B^+}} \cdot \frac{Br(B^+ \rightarrow \phi K_1(1400)^+)}{BR(B^0 \rightarrow \phi K_1(1400)^0)} = \begin{cases} 1.03^{+0.84}_{-0.67} & \theta_{K_1} \sim 33^\circ \\ 1.07^{+0.92}_{-0.71} & \theta_{K_1} \sim 58^\circ \end{cases}, \quad (73)$$

which could be used to further determine the mixing angle θ_{K_1} and will be tested by the future precision B meson experiments.

- As seen in Table V, the annihilation diagrams have been straightforwardly and explicitly evaluated in the pQCD approach. Furthermore, one can easily find out the large annihilation contributions in the considered $B \rightarrow \phi K_1$ decays. Therefore, whether the annihilation effects to these decay modes is important or not can be determined by the future precise measurements experimentally, which will provide useful hints to understand the annihilation decay mechanism in B meson physics and identify the reliability of investigations in these kinds of decays by employing the pQCD approach. Frankly speaking, these branching ratios for the $B \rightarrow \phi K_1$ decays predicted in the pQCD approach suffer relatively large uncertainties from the currently less constrained hadronic parameters of the strange axial-vector K_{1A} and K_{1B} states, which needs further improvements from future experiments.

TABLE V. The decay amplitudes(in unit of 10^{-3} GeV^3) of the $B^+ \rightarrow \phi K_{1A}^+$ and $B^+ \rightarrow \phi K_{1B}^+$ modes with three polarizations in the pQCD approach, where only the central values are quoted for clarification.

Decay Amplitudes	\mathcal{A}_{fe}^T	\mathcal{A}_{fe}^P	\mathcal{A}_{nfe}^T	\mathcal{A}_{nfe}^P	\mathcal{A}_{nfa}^T	\mathcal{A}_{nfa}^P	\mathcal{A}_{fa}^T	\mathcal{A}_{fa}^P
Channel	$B^+ \rightarrow \phi K_{1A}^+$							
L	0.0	-4.51	0.0	0.45 - i 0.11	0.04 - i 0.02	0.01 - i 0.03	-0.05 + i 0.14	0.88 - i 0.91
N	0.0	-0.85	0.0	-0.32 - i 0.10	~ 0.00	-0.03 + i 0.03	0.15 + i 0.25	0.51 - i 2.13
T	0.0	-1.66	0.0	-0.71 - i 0.10	-0.01 + i 0.01	-0.06 + i 0.08	-0.31 - i 0.51	-1.92 - i 3.47
Channel	$B^+ \rightarrow \phi K_{1B}^+$							
L	0.0	6.35	0.0	-0.23 + i 0.17	0.02 - i 0.06	-0.04 - i 0.04	-0.21 - i 0.23	-1.96 - i 0.67
N	0.0	0.64	0.0	0.22 + i 0.55	~ 0.00	-0.03 + i 0.02	0.07 + i 0.05	-0.19 - i 0.57
T	0.0	1.31	0.0	0.48 + i 1.11	-0.01 + i 0.01	-0.04 + i 0.07	-0.14 - i 0.13	-1.12 - i 0.61

B. CP-averaged polarization fractions and relative phases

Now we come to the analysis of the polarization fractions for $B \rightarrow \phi K_1$ decays in the pQCD approach. Based on the helicity amplitudes, we can define the transversity amplitudes,

$$\mathcal{A}_L = \lambda m_B^2 \mathcal{M}_L, \quad \mathcal{A}_{||} = \lambda \sqrt{2} m_B^2 \mathcal{M}_N, \quad \mathcal{A}_\perp = \lambda m_\phi m_{K_1} \sqrt{2(r^2 - 1)} \mathcal{M}_T. \quad (74)$$

for the longitudinal, parallel, and perpendicular polarizations, respectively, with the normalization factor $\lambda = \sqrt{G_F^2 P_c / (16\pi m_B^2 \Gamma)}$ and the ratio $r = P_2 \cdot P_3 / (m_\phi \cdot m_{K_1})$. These amplitudes satisfy the relation,

$$|\mathcal{A}_L|^2 + |\mathcal{A}_\parallel|^2 + |\mathcal{A}_\perp|^2 = 1 \quad (75)$$

following the summation in Eq. (63). Since the transverse-helicity contributions manifest themselves in polarization observables, we therefore define one kind of the polarization observables, i.e., polarization fractions $f_{L,\parallel,\perp}$ as,

$$f_{L,\parallel,\perp} = \frac{|\mathcal{A}_{L,\parallel,\perp}|^2}{|\mathcal{A}_L|^2 + |\mathcal{A}_\parallel|^2 + |\mathcal{A}_\perp|^2}, \quad (76)$$

With the above transversity amplitudes, the relative phases ϕ_\parallel and ϕ_\perp can be defined as

$$\phi_\parallel = \arg \frac{\mathcal{A}_\parallel}{\mathcal{A}_L}, \quad \phi_\perp = \arg \frac{\mathcal{A}_\perp}{\mathcal{A}_L}, \quad (77)$$

The theoretical results of polarization fractions and relative phases for these considered $B \rightarrow \phi K_1$ decays in the pQCD approach have been displayed in Tables I-IV. Based on these numerical values, some comments are given as follows:

- Theoretically, the pQCD predictions of the longitudinal polarization fraction f_L for the $B^+ \rightarrow \phi K_1(1270)^+$ mode are

$$f_L(B^\pm \rightarrow \phi K_1(1270)^\pm)_{\text{pQCD}} = \begin{cases} 0.47_{-0.32}^{+0.31} & \theta_{K_1} \sim 33^\circ \\ 0.11_{-0.07}^{+0.11} & \theta_{K_1} \sim 58^\circ \end{cases}, \quad (78)$$

Experimentally, the longitudinal polarization fraction f_L for the charged $B^+ \rightarrow \phi K_1(1270)^+$ decay is now available [2],

$$f_L(B^\pm \rightarrow \phi K_1(1270)^\pm)_{\text{Exp.}} = 0.46_{-0.15}^{+0.13}, \quad (79)$$

It is obvious to see that the fraction with the smaller angle $\theta_{K_1} \sim 33^\circ$ is well consistent with the current data, which will be further examined by the LHCb and/or Super-B measurements in the near future.

- In Refs. [9, 11], the authors have also evaluated the polarization fraction of the $B^+ \rightarrow \phi K_1(1270)^+$ decays by employing GFA and QCDF, respectively. However, it is noted that the longitudinal fraction predicted in GFA is 91.9%(85.7%) [11] with the mixing angle $\theta_{K_1} \sim 37^\circ(58^\circ)$, which, in terms of the central value, is almost two times larger than the measured one. As seen in Table I, the theoretical predictions for the longitudinal polarization fraction of $B^+ \rightarrow \phi K_1(1270)^+$ decay in QCDF and pQCD approaches are consistent with the current observation within still large errors.
- For other three $B \rightarrow \phi K_1$ decays, the longitudinal polarization fractions have also been predicted in GFA, QCDF, and pQCD, respectively. From the numerical results shown in Tables I-IV, it is interesting to find that the theoretical predictions of the longitudinal polarization fractions for the $B \rightarrow \phi K_1(1270)$ decays are more sensitive than those for the $B \rightarrow \phi K_1(1400)$ decays to the variation of the mixing angle θ_{K_1} in both QCDF and pQCD approaches, which is contrary to that observed in GFA [11]: 91.9%(85.7%) for $B \rightarrow \phi K_1(1270)$ decays and 79.2%(99.5%) for $B \rightarrow \phi K_1(1400)$ decays with the mixing angle $\theta_{K_1} \sim 37^\circ(58^\circ)$. The above predictions and relevant phenomenologies will be tested by future measurements at LHC and/or Super-B experiments.
- Up to now, there are no any available data and theoretical predictions on the relative phases(in unit of rad) ϕ_\parallel and ϕ_\perp of the $B \rightarrow \phi K_1$ decays yet. It is therefore expected that our predictions in the pQCD approach for the relative phases of these considered $B \rightarrow \phi K_1$ decays as given in Tables I-IV will be tested by the future LHCb and/or Super-B experiments.

C. Direct CP-violating asymmetries

Now we come to the evaluations of the CP-violating asymmetries of $B \rightarrow \phi K_1$ decays in the pQCD approach. For the charged B meson decays, the direct CP violation $\mathcal{A}_{CP}^{\text{dir}}$ can be defined as,

$$\mathcal{A}_{CP}^{\text{dir}} = \frac{|\overline{\mathcal{A}}_f|^2 - |\mathcal{A}_f|^2}{|\overline{\mathcal{A}}_f|^2 + |\mathcal{A}_f|^2}, \quad (80)$$

where \mathcal{A}_f stands for the decay amplitude of $B^+ \rightarrow \phi K_1^+$, while $\bar{\mathcal{A}}_f$ denotes the charge conjugation one correspondingly. Using Eq. (80), we find the following pQCD predictions of the direct CP-violating asymmetries

$$\mathcal{A}_{CP}^{\text{dir}}(B^+ \rightarrow \phi K_1(1270)^+)_{\text{pQCD}} = \begin{cases} -0.7^{+3.6}_{-2.9} \times 10^{-2} & \theta_{K_1} \sim 33^\circ \\ -1.3^{+1.1}_{-0.8} \times 10^{-2} & \theta_{K_1} \sim 58^\circ \end{cases}, \quad (81)$$

$$\mathcal{A}_{CP}^{\text{dir}}(B^+ \rightarrow \phi K_1(1400)^+)_{\text{pQCD}} = \begin{cases} -1.5^{+1.2}_{-1.5} \times 10^{-2} & \theta_{K_1} \sim 33^\circ \\ -1.3^{+1.5}_{-1.7} \times 10^{-2} & \theta_{K_1} \sim 58^\circ \end{cases}; \quad (82)$$

in which various errors as specified previously have been added in quadrature. One can easily see that the direct CP asymmetries of those two charged $B \rightarrow \phi K_1$ decays are around $-3.6\% \sim +2.9\%$ ($-2.1\% \sim -0.2\%$) and $-3.0\% \sim -0.3\%$ ($-3.0\% \sim +0.2\%$) with the mixing angle $\theta_{K_1} \sim 33^\circ(58^\circ)$, respectively. Note that these two channels exhibit much small direct CP-violating asymmetries in the pQCD approach since the contributions coming from the tree operators are approximately neglected in these two charged $B^+ \rightarrow \phi K_1^+$ decays relative to the dominant penguin contributions, which can be clearly seen from the decay amplitudes of every topology as shown in Table V.

At the experimental aspect, as mentioned in the Introduction, the BABAR Collaboration has reported the measurements of the direct CP violation for $B^\pm \rightarrow \phi K_1(1270)^\pm$ mode,

$$\mathcal{A}_{CP}^{\text{dir}}(B^\pm \rightarrow \phi K_1(1270)^\pm)_{\text{Exp.}} = (-15.0 \pm 20.0) \times 10^{-2}, \quad (83)$$

which is consistent with our pQCD calculations as shown in Eq. (81) within errors. It is worth of stressing that the preliminary measurements by BABAR Collaboration suffer from large statistical and systematic errors. One need more data from other experiments such as LHC and Super-B to improve the precision of the direct CP asymmetry of $B^+ \rightarrow \phi K_1^+$ decays.

Meanwhile, by combining three polarization fractions in the transversity basis with those of its CP-conjugated \bar{B} decays, we also computed the direct CP violations of $B^+ \rightarrow \phi K_1^+$ decays in every polarization in the pQCD approach for tests by future experimental measurements. The direct CP asymmetries of $B^+ \rightarrow \phi K_1^+$ decays in the transversity basis can be defined as,

$$\mathcal{A}_{CP}^{\text{dir},\alpha} = \frac{\bar{f}_\alpha - f_\alpha}{f_\alpha + f_\alpha}, \quad (84)$$

where $\alpha = L, \parallel, \perp$ and the definition of \bar{f} is same as that in Eq.(76) but for the corresponding \bar{B} decays. The numerical results for the direct CP asymmetries of $B^+ \rightarrow \phi K_1^+$ decays in the transversity basis within the framework of pQCD approach are presented in Table I and II, where the various errors as specified previously have also been added in quadrature.

As for the CP-violating asymmetries for the neutral $B^0 \rightarrow \phi K_1^0$ decays, the effects of $B^0 - \bar{B}^0$ mixing should be considered. However, since they involve the pure penguin contributions at leading order in the SM, which can be seen from the decay amplitudes as given in Eq. (60), the considered two neutral modes then present no direct CP violations in the SM. If the measurements from experiments for the direct CP asymmetries $\mathcal{A}_{CP}^{\text{dir}}$ in $B^0 \rightarrow \phi K_1(1270)^0$ and $\phi K_1(1400)^0$ decays exhibit large nonzero values, which will indicate the existence of new physics beyond the SM and will provide a very promising place to look for this exotic effect.

D. Effects of annihilation contributions

As discussed in Ref. [9], the weak annihilation contributions play a more important role in $B \rightarrow \phi K_1(1400)$ decays than that in $B \rightarrow \phi K_1(1270)$ decays. At last, we will therefore explore the important contributions from the weak annihilation diagrams to the penguin-dominated $B \rightarrow \phi K_1$ decays considered in this work. In Tables VI and VII, we present the central values of the pQCD predictions for the CP-averaged branching ratios, the polarization fractions, the relative phases and the direct CP-violating asymmetries with mixing angles $\theta_{K_1} \sim 33^\circ$ and $\theta_{K_1} \sim 58^\circ$ by taking the following three different sets of decay amplitudes into account:

- (1) The factorizable emission diagrams only (the first entry);
- (2) The factorizable emission plus the weak annihilation contributions (the second entry);
- (3) The factorizable emission plus the non-factorizable emission contributions (the third entry).

Then some phenomenological discussions are given as the following:

- Generally speaking, by combining the analytic expressions as shown in Eqs. (59-60) and the numerical results of the decay amplitudes as presented in Table V of $B^+ \rightarrow \phi K_1^+$ decays, it is clear to see that the $B^+ \rightarrow \phi K_1(1400)^+$ decay will be significantly dominated by the factorizable emission diagrams with both $\theta_{K_1} \sim 33^\circ$ and $\theta_{K_1} \sim 58^\circ$, while the

TABLE VI. The pQCD predictions for the CP-averaged branching ratios and other physical observables for the considered $B \rightarrow \phi K_1$ decays with the inclusion of the contributions from different sources as described in text. Here only the central values are quoted for clarification with the mixing angle $\theta_{K_1} \sim 33^\circ$.

	decay rates	polarization fractions			relative phases		direct CP asymmetries			
Decay modes	$\text{BR}(10^{-6})$	f_L	f_{\parallel}	f_{\perp}	$\phi_{\parallel}(\text{rad})$	$\phi_{\perp}(\text{rad})$	$\mathcal{A}_{CP}^{\text{dir}}$	$\mathcal{A}_{CP}^{\text{dir,L}}$	$\mathcal{A}_{CP}^{\text{dir},\parallel}$	$\mathcal{A}_{CP}^{\text{dir},\perp}$
$B^+ \rightarrow \phi K_1(1270)^+$	4.7	1.0	~ 0.0	~ 0.0	π	π	0.0	0.0	0.0	0.0
	7.5	0.34	0.39	0.27	2.19	3.08	~ 0.0	0.05	-0.25	0.29
	5.3	0.93	0.04	0.04	4.49	4.45	0.0	0.0	0.0	0.0
$B^0 \rightarrow \phi K_1(1270)^0$	4.4	1.0	~ 0.0	~ 0.0	π	π	0.0	0.0	0.0	0.0
	7.0	0.30	0.43	0.27	2.33	4.69	0.0	0.0	0.0	0.0
	5.0	0.93	0.04	0.04	4.50	4.46	0.0	0.0	0.0	0.0
$B^+ \rightarrow \phi K_1(1400)^+$	32.0	0.93	0.04	0.03	π	π	0.0	0.0	0.0	0.0
	23.6	0.73	0.12	0.15	4.24	3.77	-0.01	-0.01	-0.23	0.14
	30.4	0.85	0.08	0.07	3.37	3.34	0.0	0.0	0.0	0.0
$B^0 \rightarrow \phi K_1(1400)^0$	29.6	0.93	0.04	0.03	π	π	0.0	0.0	0.0	0.0
	20.9	0.71	0.13	0.16	4.31	3.76	0.0	0.0	0.0	0.0
	28.2	0.85	0.08	0.07	3.38	3.34	0.0	0.0	0.0	0.0

$B^+ \rightarrow \phi K_1(1270)^+$ decay will be strongly determined by the annihilation diagrams with the increasing of the mixing angle from $\theta_{K_1} \sim 33^\circ$ to $\theta_{K_1} \sim 58^\circ$. These observations have been confirmed through the central values of the CP-averaged branching ratios in the pQCD approach as displayed in Tables VI-VII. Of course, the similar phenomena will occur in the neutral $B^0 \rightarrow \phi K_1^0$ decays because of the negligible contributions induced by the tree operators in the charged $B^+ \rightarrow \phi K_1^+$ decays.

- As far as the branching ratios are considered, one can see from Table VI-VII that the annihilation diagrams contribute to $B \rightarrow \phi K_1(1270)$ decays less(much larger) than those to $B \rightarrow \phi K_1(1400)$ decays with $\theta_{K_1} \sim 33^\circ(58^\circ)$. More explicitly, without the annihilation contributions, the branching ratios of $B \rightarrow \phi K_1(1400)$ modes become larger by about 21% \sim 25% with $\theta_{K_1} \sim 33^\circ$. However, by neglecting the weak annihilation contributions, the branching ratios of $B \rightarrow \phi K_1(1270)$ decays decrease near 92%, while those of $B \rightarrow \phi K_1(1400)$ decays increase around 63% \sim 75% with $\theta_{K_1} \sim 58^\circ$.
- For the polarization fractions and relative phases, one can also see that the annihilation contributions play an important role in all the considered $B \rightarrow \phi K_1$ decays. It is interesting to find that, analogous to $B \rightarrow \phi K^*$ decays, the weak annihilation contributions could also reduce the longitudinal polarization of the $B \rightarrow \phi K_1$ decays significantly. While the non-factorizable emission diagrams play a minor role for these quantities.
- Moreover, as claimed in the pQCD approach, the annihilation diagrams provide the origin of the strong phases for predicting the CP violation in the considered $B \rightarrow \phi K_1$ decays in the present work, which can be seen obviously from the numerical values presented in Tables VI and VII. Of course, the above general expectation for the pQCD approach will be examined by the relevant experiments in the future, which could be helpful to understand the annihilation decay mechanism in vector-vector and vector-axial-vector B decays in depth.

IV. CONCLUSIONS AND SUMMARY

In this work, we studied the charmless hadronic $B \rightarrow \phi K_1$ decays, which are dominated by the penguin contributions, by employing the pQCD approach based on the framework of k_T factorization theorem. By taking the mixing angles $\theta_{K_1} \sim 33^\circ$ and $\theta_{K_1} \sim 58^\circ$ between the two axial-vector $K_1(1270)$ and $K_1(1400)$ mesons, we explored the physical observables such as the CP-averaged branching ratios, the polarization fractions, the relative phases, and the CP-violating asymmetries of the considered decay modes.

From our numerical and phenomenological studies we found the following points:

TABLE VII. Same as Table VI but with mixing angle $\theta_{K_1} \sim 58^\circ$.

	decay rates	polarization fractions			relative phases		direct CP asymmetries			
Decay modes	BR(10^{-6})	f_L	f_{\parallel}	f_{\perp}	$\phi_{\parallel}(\text{rad})$	$\phi_{\perp}(\text{rad})$	$\mathcal{A}_{CP}^{\text{dir}}$	$\mathcal{A}_{CP}^{\text{dir,L}}$	$\mathcal{A}_{CP}^{\text{dir,}\parallel}$	$\mathcal{A}_{CP}^{\text{dir,}\perp}$
$B^+ \rightarrow \phi K_1(1270)^+$	0.4	0.30	0.41	0.29	π	π	0.0	0.0	0.0	0.0
	10.4	0.11	0.47	0.42	3.59	2.96	-0.01	0.15	-0.26	0.23
	0.7	0.03	0.52	0.44	2.76	2.68	0.0	0.0	0.0	0.0
$B^0 \rightarrow \phi K_1(1270)^0$	0.4	0.29	0.41	0.29	π	π	0.0	0.0	0.0	0.0
	10.4	0.12	0.48	0.40	3.68	2.95	0.0	0.0	0.0	0.0
	0.7	0.03	0.53	0.44	2.76	2.67	0.0	0.0	0.0	0.0
$B^+ \rightarrow \phi K_1(1400)^+$	36.3	0.95	0.03	0.02	π	π	0.0	0.0	0.0	0.0
	20.8	0.90	0.04	0.06	3.99	3.75	-0.01	-0.01	-0.13	0.06
	34.9	0.88	0.07	0.06	3.48	3.46	0.0	0.0	0.0	0.0
$B^0 \rightarrow \phi K_1(1400)^0$	33.6	0.95	0.03	0.02	π	π	0.0	0.0	0.0	0.0
	17.7	0.89	0.04	0.07	4.06	3.76	0.0	0.0	0.0	0.0
	32.4	0.88	0.07	0.05	3.49	3.46	0.0	0.0	0.0	0.0

- (a) The pQCD predictions for the branching ratio, the polarization fractions, and the direct CP asymmetry of the $B^\pm \rightarrow \phi K_1(1270)^\pm$ decay with the mixing angle $\theta_{K_1} \sim 33^\circ$ are in good agreement with the current data as reported by the BABAR Collaboration, which suggests that the small mixing angle $\theta_{K_1} \sim 33^\circ$ is possibly more favored.
- (b) For $B^\pm \rightarrow \phi K_1(1400)^\pm$ decay, however, the pQCD predictions for its decay rate with two different mixing angles basically agrees with the ones in the QCDF approach within still large theoretical errors, but much larger than the preliminary upper limit set by the BABAR Collaboration, which will be tested by the LHCb and forthcoming Super-B experiments. Of course, the numerical results in pQCD approach are consistent with the available upper limit roughly in 2σ errors.
- (c) At the theoretical aspect, only parts of the numerical results predicted in every different method or approach can be accommodated by the preliminary data. Once the measurements reported by BABAR Collaboration would be confirmed by the future measurements, it will be of great interest and probably a challenge to further understand the K_1 hadrons' QCD behavior and the mixing angle θ_{K_1} between two axial-vector K_{1A} and K_{1B} states.
- (d) The theoretical estimations on the relative phases and direct CP-violating asymmetries of penguin-dominant $B \rightarrow \phi K_1$ decays are given for the first time in the pQCD approach, which can also be tested by the experimental measurements in the near future.
- (e) The weak annihilation contributions play an important role in $B \rightarrow \phi K_1(1270)$ and $\phi K_1(1400)$ decays.

The pQCD studies for the four $B \rightarrow \phi K_1$ decays will be helpful for us to understand the mixing angle θ_{K_1} , the underlying helicity structure of the decay mechanism, even the possible new physics effects in this type of decays. We believe that many pQCD predictions presented in this paper will be tested in the near future, when precision experimental measurements become available.

ACKNOWLEDGMENTS

This work is supported by the National Natural Science Foundation of China under Grants No. 11205072 and No. 11235005, and by a project funded by the Priority Academic Program Development of Jiangsu Higher Education Institutions (PAPD), by the Research Fund of Jiangsu Normal University under Grant No. 11XLR38, and by the Foundation of Yantai University under Grant No. WL07052.

-
- [1] H. -Y. Cheng, PoS Hadron **2013**, 090 (2014) [arXiv:1311.2370 [hep-ph]].
[2] B. Aubert *et al.* [BABAR Collaboration], Phys. Rev. Lett. **101**, 161801 (2008) [arXiv:0806.4419 [hep-ex]].

- [3] B. Aubert *et al.* [BABAR Collaboration], Phys. Rev. Lett. **91**, 171802 (2003) [hep-ex/0307026].
- [4] B. Aubert *et al.* [BABAR Collaboration], Phys. Rev. Lett. **93**, 231804 (2004) [hep-ex/0408017].
- [5] B. Aubert *et al.* [BABAR Collaboration], Phys. Rev. Lett. **98**, 051801 (2007) [hep-ex/0610073].
- [6] B. Aubert *et al.* [BABAR Collaboration], Phys. Rev. Lett. **99**, 201802 (2007) [arXiv:0705.1798 [hep-ex]].
- [7] K.F. Chen *et al.* [Belle Collaboration], Phys. Rev. Lett. **91**, 201801 (2003) [hep-ex/0307014].
- [8] K.F. Chen *et al.* [Belle Collaboration], Phys. Rev. Lett. **94**, 221804 (2005) [hep-ex/0503013].
- [9] H.Y. Cheng and K.C. Yang, Phys. Rev. D **78**, 094001 (2008) [Erratum-ibid. D **79**, 039903 (2009)] [arXiv:0805.0329 [hep-ph]].
- [10] G. Calderon, J.H. Munoz and C.E. Vera, Phys. Rev. D **76**, 094019 (2007) [arXiv:0705.1181 [hep-ph]].
- [11] C.H. Chen, C.Q. Geng, Y.K. Hsiao and Z.T. Wei, Phys. Rev. D **72**, 054011 (2005) [hep-ph/0507012].
- [12] G. Valencia, Phys. Rev. D **39**, 3339 (1989).
- [13] A. Datta and D. London, Int. J. Mod. Phys. A **19**, 2505 (2004) [hep-ph/0303159].
- [14] G. Buchalla, A.J. Buras and M.E. Lautenbacher, Rev. Mod. Phys. **68**, 1125 (1996) [hep-ph/9512380].
- [15] Y.Y. Keum, H.-n. Li and A.I. Sanda, Phys. Lett. B **504**, 6 (2001) [hep-ph/0004004].
- [16] Y.Y. Keum, H.-n. Li and A.I. Sanda, Phys. Rev. D **63**, 054008 (2001) [hep-ph/0004173].
- [17] C.D. Lü, K. Ukai and M.Z. Yang, Phys. Rev. D **63**, 074009 (2001) [hep-ph/0004213].
- [18] H.-n. Li, Prog. Part. Nucl. Phys. **51**, 85 (2003) [hep-ph/0303116].
- [19] C.M. Arnesen, Z. Ligeti, I.Z. Rothstein and I.W. Stewart, Phys. Rev. D **77**, 054006 (2008) [hep-ph/0607001].
- [20] J. Chay, H.-n. Li and S. Mishima, Phys. Rev. D **78**, 034037 (2008) [arXiv:0711.2953 [hep-ph]].
- [21] C.D. Lu and K. Ukai, Eur. Phys. J. C **28**, 305 (2003) [hep-ph/0210206].
- [22] Y. Li, C.D. Lu, Z.J. Xiao and X.Q. Yu, Phys. Rev. D **70**, 034009 (2004) [hep-ph/0404028].
- [23] A. Ali, G. Kramer, Y. Li, C.D. Lu, Y.L. Shen, W. Wang and Y.M. Wang, Phys. Rev. D **76**, 074018 (2007) [hep-ph/0703162].
- [24] Z.J. Xiao, W.F. Wang and Y.Y. Fan, Phys. Rev. D **85**, 094003 (2012) [arXiv:1111.6264 [hep-ph]].
- [25] B.H. Hong and C.D. Lu, Sci. China G **49**, 357 (2006) [hep-ph/0505020].
- [26] H.-n. Li and S. Mishima, Phys. Rev. D **71**, 054025 (2005) [hep-ph/0411146].
- [27] H.-n. Li, Phys. Lett. B **622**, 63 (2005) [hep-ph/0411305].
- [28] H.-n. Li and H.L. Yu, Phys. Rev. Lett. **74**, 4388 (1995) [hep-ph/9409313].
- [29] H.-n. Li and H.L. Yu, Phys. Lett. B **353**, 301 (1995).
- [30] H.-n. Li and H.L. Yu, Phys. Rev. D **53**, 2480 (1996) [hep-ph/9411308].
- [31] H.-n. Li, Phys. Rev. D **66**, 094010 (2002) [hep-ph/0102013].
- [32] H.-n. Li and K. Ukai, Phys. Lett. B **555**, 197 (2003) [hep-ph/0211272].
- [33] J. Botts and G.F. Sterman, Nucl. Phys. B **325**, 62 (1989).
- [34] H.-n. Li and G.F. Sterman, Nucl. Phys. B **381**, 129 (1992).
- [35] C.D. Lu and M.Z. Yang, Eur. Phys. J. C **28**, 515 (2003) [hep-ph/0212373].
- [36] P. Ball, V.M. Braun, Y. Koike and K. Tanaka, Nucl. Phys. B **529**, 323 (1998) [hep-ph/9802299].
- [37] P. Ball and G.W. Jones, J. High Energy Phys. **0703**, 069 (2007) [hep-ph/0702100].
- [38] K.C. Yang, Nucl. Phys. B **776**, 187 (2007) [arXiv:0705.0692 [hep-ph]].
- [39] R.H. Li, C.D. Lu and W. Wang, Phys. Rev. D **79**, 034014 (2009) [arXiv:0901.0307 [hep-ph]].
- [40] J. Beringer *et al.* [Particle Data Group Collaboration], Phys. Rev. D **86**, 010001 (2012).
- [41] P. Ball and R. Zwicky, Phys. Rev. D **71**, 014029 (2005) [hep-ph/0412079].
- [42] C.H. Chen, Y.Y. Keum and H.-n. Li, Phys. Rev. D **66**, 054013 (2002) [hep-ph/0204166].
- [43] M. Suzuki, Phys. Rev. D **47**, 1252 (1993).
- [44] L. Burakovsky and J.T. Goldman, Phys. Rev. D **56**, 1368 (1997) [hep-ph/9703274].
- [45] H.Y. Cheng, Phys. Rev. D **67**, 094007 (2003) [hep-ph/0301198].
- [46] H. Hatanaka and K.C. Yang, Phys. Rev. D **77**, 094023 (2008) [Erratum-ibid. D **78**, 059902 (2008)] [arXiv:0804.3198 [hep-ph]].
- [47] H.Y. Cheng, Phys. Lett. B **707**, 116 (2012) [arXiv:1110.2249 [hep-ph]].
- [48] F. Divotgey, L. Olbrich and F. Giacosa, Eur. Phys. J. A **49**, 135 (2013) [arXiv:1306.1193 [hep-ph]].
- [49] H. G. Blundell, hep-ph/9608473.